FINAL SCIENTIFIC/TECHNICAL REPORT

Submitted To:

U.S. Department of Energy
Office of Fossil Energy and Carbon Management
National Energy Technology Laboratory

Award # DE-FE0032011

Project Title:

Titanium-Cerium Electrode-Decoupled Redox Flow Batteries Integrated With Fossil Fuel Assets For Load-Following, Long-Duration Energy Storage

Principal Investigator:

Vijay K. Ramani, Professor
Phone: 314-935-7924
Email: ramani@wustl.edu

Submission Date: July 15, 2024

UEI Number: L6NFUM28LQM5

Recipient Organization:

Washington University
One Brookings Dr.
Saint Louis, MO 63130

Project/Grant Period: 03/01/2021 – 02/29/2024

Final Scientific/Technical Report

Contributing Authors

Benjamin Kumfer[a]
Shrihari Sankarasubramanian[b]
Matthew Kastelic[c]
Judith Lattimer[c]
Vijay Ramani[a]

a Dept. Energy, Environmental & Chemical Engineering, Washington University in St. Louis, USA
b Dept. Biomedical & Chemical Engineering, University of Texas San Antonio, USA
c Giner Labs, Newton MA, USA

Acknowledgment: This material is based upon work supported by the Department of Energy National Energy Technology Lab under Award Number(s) DE-FE0032011.

TABLE OF CONTENTS

LIST OF FIGURES

1. Executive Summary

Operation of fossil plants at partial capacity with frequent cycling results in decreased efficiency, increased emissions and increased wear and maintenance. The objective of this project is to advance the integration of a titanium-cerium electrode-decoupled redox flow battery (RFB) system with conventional fossil-fueled power plants through technical and economic system-level studies and component scale-up and R&D. The Ti-Ce chemistry has a pathway to meet the DOE cost targets of $100/kWh and $0.05/kWh-cycle owing to the use of low-cost, earth abundant elemental actives and incorporation of inexpensive carbon felt electrodes and non-fluorinated anion exchange membrane (AEM) separators. The initial unit cell design was scaled up, with some modifications made to improve ease of manufacturing, from 25 cm^2 cell area to 400 cm^2. Electrochemical tests demonstrated operation at a current density up to 50 mA/cm^2, which is on par with other commercial RFB offerings. Furthermore, the Ti-Ce technology developed by WashU was evaluated and tested by industrial team partner, Giner, Inc., in their modular 3-cell stack. Several cell design modifications and alternate component material selections were successfully implemented to accommodate this chemistry while reducing polarization and leakage. Results from stack testing show high columbic efficiency and indicate that further optimization of cell compression and components will lead to successful operation of the Ti-Ce ED-RFB over longer duration at the multi-cell stack level. Engineering and cost analysis showed that an RFB system with power output on the order of 100 MW and with a charge/discharge duration of approx. 12 hours is the most cost effective for integration with fossil plants. At this scale, projected cycling of fossil fuel power plants can be significantly reduced. The use of a storage system is shown to reduce the fossil plant standalone cost of electricity by $7/MWh, through increased capacity factor and improved average efficiency, in the scenario of high penetration of renewable power.

2. Project Overview

2.1 Background

This project aims to improve the U.S. fleet of fossil-fueled power plants through direct integration of a titanium-cerium electrode-decoupled redox flow battery (Ti-Ce ED-RFB) system for large scale energy storage. The penetration of intermittent wind and solar electricity sources onto power grids has led to an increase in cycling of pulverized coal (PC) and natural gas combined cycle (NGCC) plants to match load [1-3]. Most of these plants were designed to provide steady baseload power with a high capacity factor; operation at partial capacity results in a substantial decrease in plant efficiency. Ramping and operating away from optimal efficiency can also result in increasing emissions(4). Furthermore, incidents of damage to steam components from creep and fatigue have been attributed to the increase of plant cycling, leading to rising maintenance costs and outages, and a reduction in component lifespan[4-6].

The Energy Information Agency projects that the share of U.S. electricity generation from renewable sources will rise from 18% to 31% by 2050 due to the addition of more intermittent wind and solar PV sources[7]. Meanwhile, incidents of excess wind energy curtailment and negative locational marginal pricing (LMP) in the U.S. have already been widely reported. Ultimately, the goal of attaining a high share of renewable power will be predicated on the availability of solutions for large-scale energy storage to prevent grid imbalances between available power and demand.

Co-location of redox flow batteries (RFBs) with fossil assets provides opportunities to increase efficiency and reduce costs through integration of heat, water, and power. The cooling needs of the RFB can be met from the power plant's cooling water supply, significantly reducing the balance of plant costs for the RFB. Other points of synergy include auxiliary power to pump the electrolytes and power conditioning of the RFB output can both be accomplished with existing power plant sub-systems.

2.2 Description of Technology

Redox flow batteries (RFBs) including the all-V, iron-based and Zn-Br chemistries have been listed as fossil asset integrated energy storage technology focus areas by the DOE OFE. (12) Redox flow battery (RFB) systems are electrochemical energy storage systems with decoupled energy and power ratings. This is achieved by the use of soluble redox active species (electrolytes) to store energy which are stored outside the body of the electrochemical reactor. Thus, the quantity of the

electrolytes determines the amount of energy a system can store while the configuration of the reactor itself (area of the electrodes, resistance, electrolyte flowrate) independently determines the power output, thus enabling the decoupling of the system energy and power. The electrochemical reactor itself typically consists of two electrically conducting (but ionically insulating) electrodes separated by a ionically conducting (but electrically insulating) separator which is typically (for standard low-temperature RFBs) made of ion conducting polymers. The electrolytes at the two electrodes are chosen based on standard reduction potential of the active species and the absolute difference in the standard reduction potential determines the maximum cell voltage of the RFB. Typical, mature RFB technologies (the ones listed by the DOE OFE as fossil asset integrated energy storage technology focus areas and as being at TRL 9) employ expensive active species like vanadium that exhibits 5 highly soluble oxidation states and use a cation exchange membrane (CEM) as the separator (allowing the free cross-over of vanadium ions from one electrode to the other). When CEMs are used in other mature RFBs like the iron-chromium chemistry, this leads to lower system energy density due to cross over of chemically different active species and deleterious capacity loss. Systems like the zinc-bromine RFBs that try to overcome this issue using one solid electrode (zinc) with a soluble active species (bromine) introduce new problems due to the formation of dendrites on the solid electrode which can eventually short circuit the RFB.

We propose an electrode-decoupled (ED-) RFB configuration using an anion exchange membrane (AEM) separator that will significantly reduce active species cross-over. This ED-RFB configuration allows us to use less expensive active materials without fear of cross-over reducing the system lifetime. One such promising technology is our novel, patent-pending Ti-Ce electrode-decoupled (i.e. different cationic active species at the anode and cathode that do not mix) redox flow battery (ED-RFBs) (14) at TRL 4 exhibiting low-cost and stability (no phase change reaction) (see Figure 2.1 for detailed schematic and half -cell reactions).

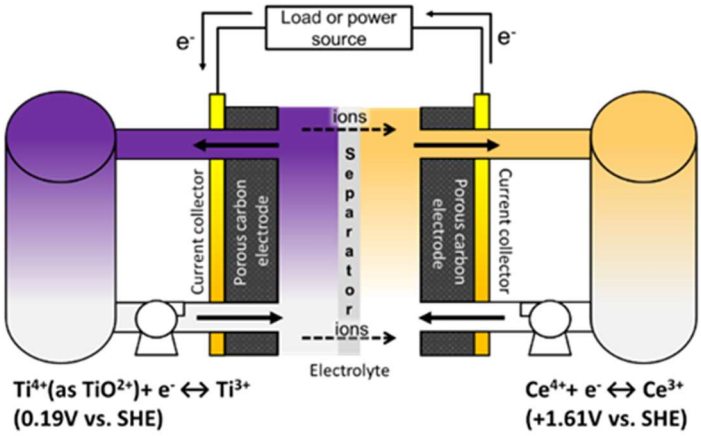

Figure 2.1 Diagram of an electrode-recoupled Ti-Ce redox flow battery.

Prior research and testing have demonstrated that the Ti-Ce system exhibits both long cycle life and allows for extended duration, demand-conformal energy storage. For additional technical information including performance data obtained prior to this project and discussion of the Technology Readiness Level (TRL), the reader is referred to the Technology Maturation Plan (Appendix 1).

2.3 Scope and Objectives

The overall project objective is to advance, through technical and economic system-level studies and component R&D and scale-up, the integration of advanced redox flow battery (RFB) systems for large scale energy storage with conventional fossil-fueled power plants. We aim to build and demonstrate a ED-RFB multi-cell stack and 400 cm^2 cells at up to 0.5 A/cm^2 current density, 48-hour cycle duration and <5% capacity loss in 1-week standby. This project seeks to advance the Technology Readiness Level (TRL) from 4 to 5. The cost and test performance of this unit will be incorporated into a techno-economic assessment (TEA) of this storage technology, integrated within the fence lines of a fossil-fueled power plant, to demonstrate a pathway to capex (capital expense) values of < $500/kW (power) and < $50/kWh (energy) for an annual production volume of > 100 MW/yr and > 1 GW h/yr and a levelized cost of storage (LCOS) of < $0.05/kWh-cycle. The TEA aims to reveal the benefits of co-location to asset owners, the grid, and the public, and will consider plants powered with natural gas, with and without carbon capture. The path to commercialization of this storage technology will be enabled through market research, gap assessment, and technology maturation and commercialization planning. The resulting assessments and performance data seeks to reduce risks and barriers to wide-scale deployment of integrated grid-scale storage, resulting in more secure, reliable, efficient, and cost-effective delivery of electricity with increased renewable share.

The project is a multi-institutional team effort led by Washington University in St. Louis. The effort to scale-up a unit cell to 400 cm^2 is led by Prof. Shrihari Sankarasubramanian at University of Texas San Antonio, who is also a co-inventor of the Ti-Ce RFB technology. The effort to provide third party validation and multi-cell stack testing is provided by Giner Labs, under the project management of Dr. Matthew Kastelic. Input relating to integration with existing power plants is provided by Tom Callahan and others at Ameren Missouri.

3. Results: Scale-Up of Unit Cell (Summary of Work Performed at UTSA)

3.1 Scale-up, Design and Fabrication Electrochemical Cell:

This task involved the scale-up of the lab-scale 25cm^2 redox flow battery (RFB) cell to a 400cm^2 single cell and to a the 4-cell stack (with each cell of 400cm^2 surface area). The initial design of electrochemical cells for both the single-cell and multi-cell stack operation of the Ti-Ce electrode-decoupled redox flow battery (ED-RFB) were completed. That initial design is shown in Figure 3.1.

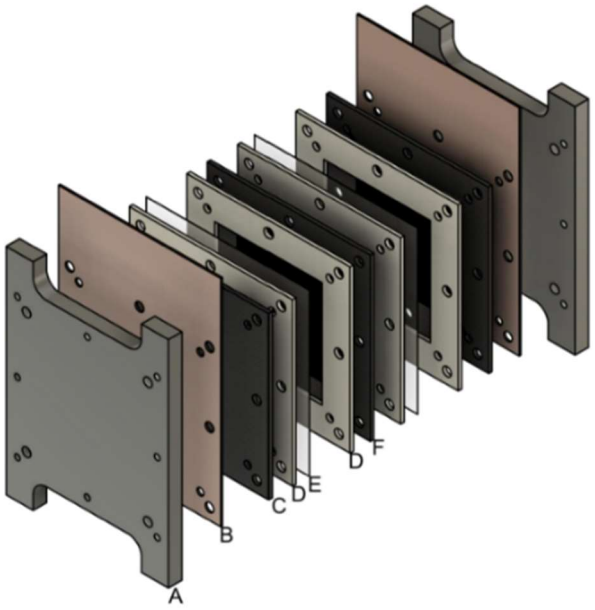

Figure 3.1 3D exploded view of laboratory stack design Figure labels - (A) back body, (B) current collector, (C) graphite monopolar plate, (D) gasket, (E) membrane assembly and (F) graphite bipolar plate.

This initial design was completed by Dr. Sankarasubramanian at WashU and, following his transition to UTSA, the scale-up tasks were transferred to UTSA. To fabricate these designs (Figure 3.2, the UTSA team contacted 8 machine shops in the San Antonio area including university machine shops and private entities. These shops were evaluated on the basis of their ability to work with graphite. Given prior experience with using water-jet cutters for the precision machining of graphite plates, machine shops with this capability were specifically sought. Two machine shops with the needed equipment and experience working with graphite were identified. The designs were shared with both machine shops, and one was down-selected on the basis of cost.

We also explored working with Delectrik Inc. (an established flow battery vendor) to design and build short stacks. Over multiple consultations with Delectrik, a plan was developed for a custom short stack suitable for this project. But we concluded that the cost of working with them to make the short stack was beyond the budget of the project and would also replicate some of the effort from Giner Inc. Thus, we stopped pursuing this second pathway.

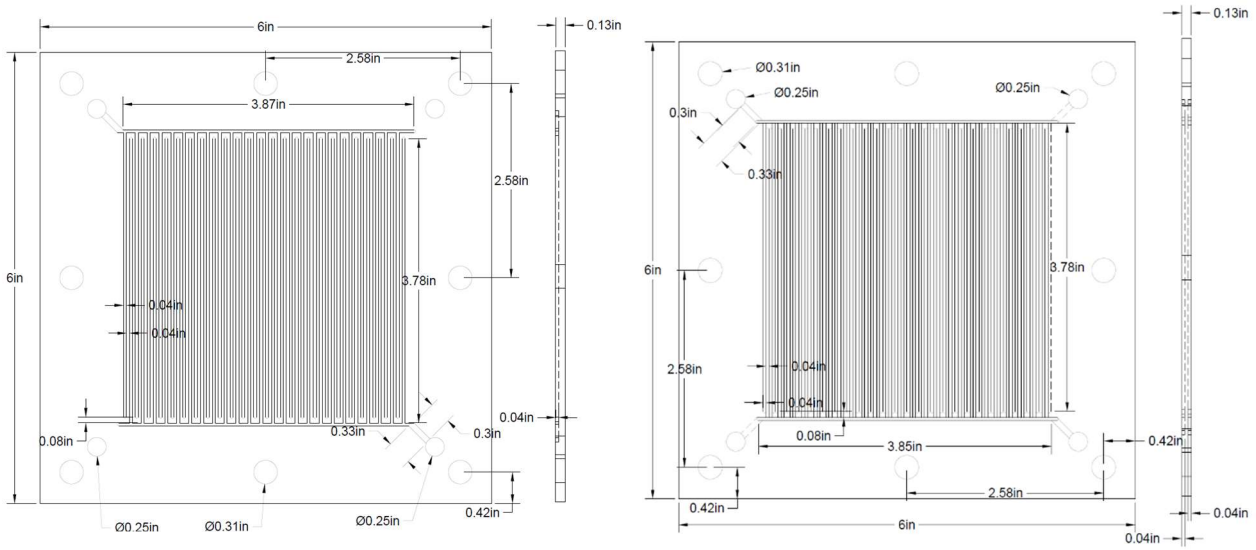

(a) (b)

Figure 3.2 (a) Monopolar flowfield design; (b) Bipolar flowfield design

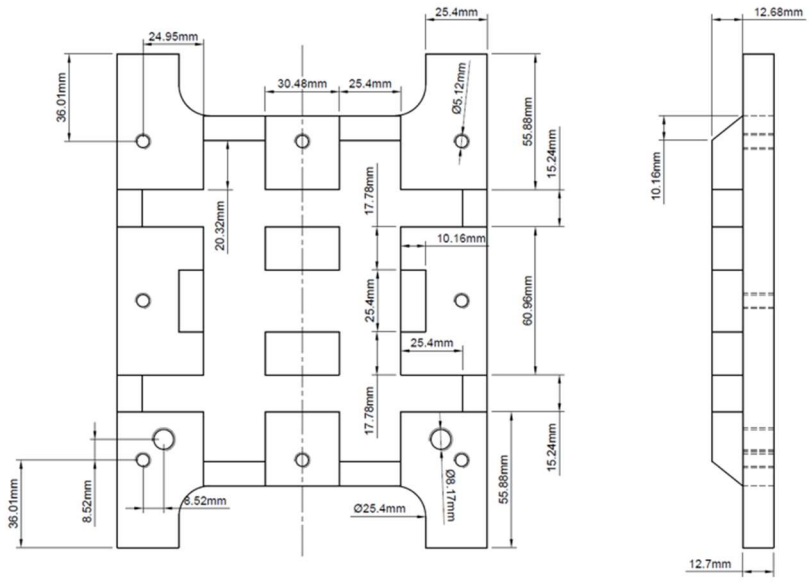

Figure 3.3 Reinforced cell/stack back body.

This task saw significant delays due to the move of the Co-PI, Shrihari Sankarasubramanian to UTSA, administrative tasks related to the sub-award and supply-chain related delays in both procuring the stack materials (impervious graphite being particularly challenging to procure) and getting it machined (several machine shops refused to accept this commission due to an order backlog). Over the course of fabrication, the grid reinforcements on the end plates (Figure 3.3) were deemed impractical and the spacing of the channels on the flowfield was found to lead to breakage of the thin channel walls during machining. Thus, the cell and stack designs were revised. Figure 3.4 and Figure 3.5 depict our revised designs for the stack and the flow fields. Given difficulties faced in making a grid design on the end plate (to possibly improve uniformity in compression) we opted for a plane design with a thicker endplate made from a higher tolerance anodized aluminum sheet. The interdigitated design of the flow field also posed challenges in machining especially at this larger surface area and thus we moved on to a flow through design. Both design modifications were not expected to significantly affect stack performance and have reduced manufacturing complexity.

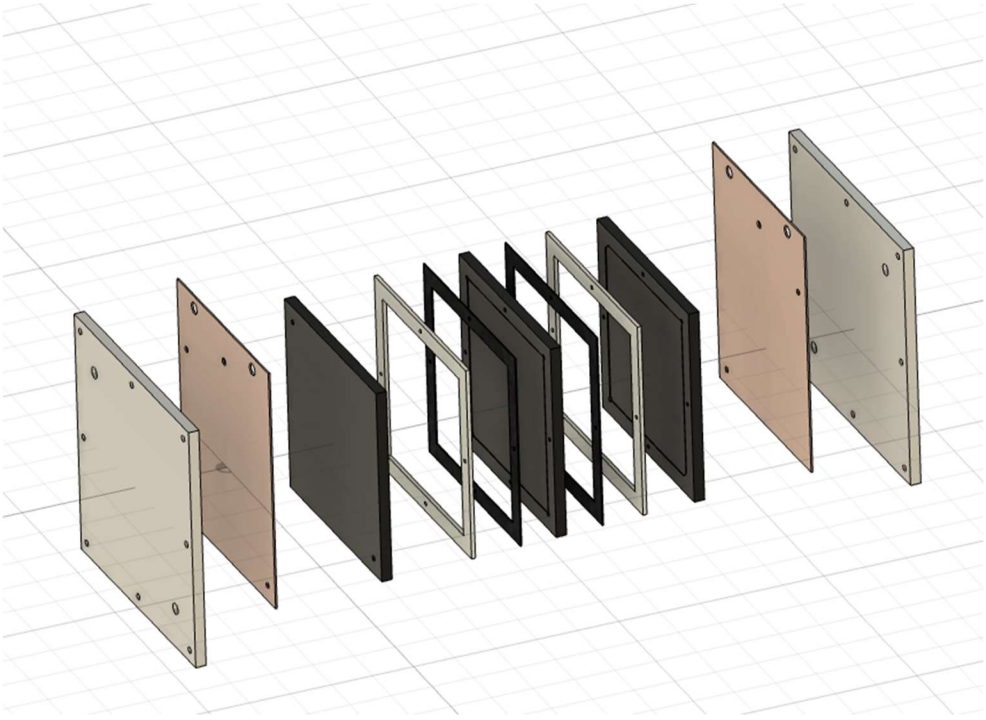

Figure 3.4 Modified stack design with no grid on the end plates and a flow-through flow field design.

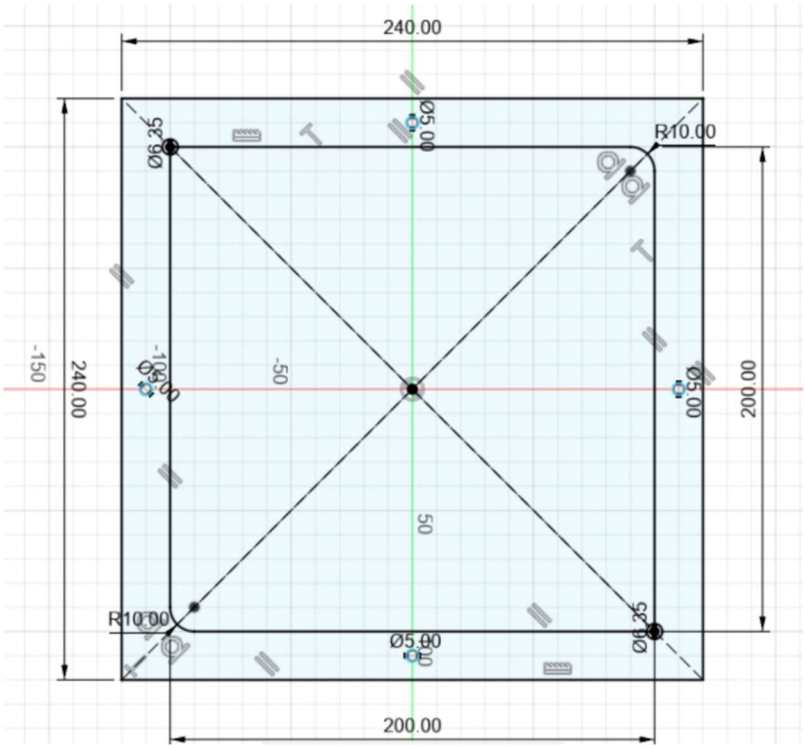

Figure 3.5 Modified flow field design with a flow-through pattern and concave edges to prevent electrolyte stagnation.

The 400 cm^2 electrochemical cell was successfully fabricated and received at UTSA (see Figure 3.6). This included bipolar plates that can be assembled with other components of this cell to yield a short stack.

Figure 3.6 Components of the 400 cm2 active area electrochemical cell and short stack

3.2 Electrochemical testing

The testing at UTSA was carried out using two different test systems depending on the scale. Initial testing was carried out using a Gamry potentiostat with the ability to output a maximum current of ±30 A and a maximum of ±20 V. We also used a ITECH source-sink power supply with the ability to charge at 170 A, discharge at 120 A and at 10 V for both operations.

The 400 cm^2 cell was initially tested for leaks using water and these tests were passed using new 400 cm^2 membranes supplied by WashU (Figure 3.8a shows assembled cell). Upon testing with acidic electrolytes, leaking started in a few hours' time preventing sustained operations. Various gasket materials (Figure 3.8b), electrolyte flowrates and felt compression ratios were tested to solve this issue.

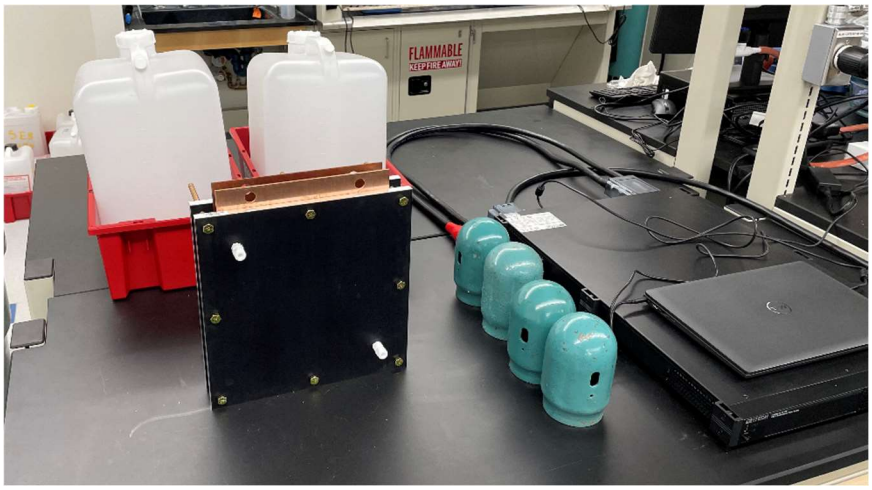

Figure 3.8a Assembled 400cm^2 active area electrochemical cell on the test bench (tanks in the background and test station to the right).

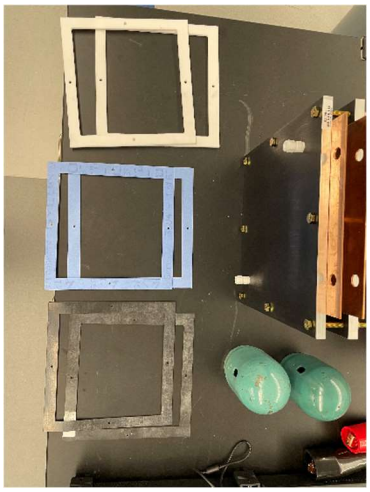

Figure 3.8b Various gasket materials (PTFE, Garlock® blue-gard style and fluoroelastomers) being evaluated for the 400cm^2 cell.

Electrochemical cycling at 20 mA/cm^2 and 50 mA/cm^2 was carried out using H_2SO_4 based electrolytes (0.5M $TiSO_4$ in 4M H_2SO_4 and 0.25M $Ce_2(SO_4)_3$ in 3M H_2SO_4). A representative cycle at 50 mA/cm^2 is shown in Figure 3.9. The high frequency resistance (HFR) of the cell was found to be significantly higher than the 25cm^2 single cell and thus the upper cutoff frequency was increased to 2.1 V. The energy efficiency was found to range from 64% to 33.4% over the course of the cycle with the 64% value being achieved across *ca* 20% of the total capacity. The high HFR of the cell precluded us from increasing the operating current density further while the electrolyte leaks prevented increasing the electrolyte volume to accommodate diurnal cycling. Given the limited budget and time to revise the cell design or accommodate additional testing, the data from the 50 mA/cm^2 cycling tests may be used in conjunction with lab-scale (25 cm^2) cells operated at the same current density to understand the scale-up effects. It is to be noted that the current density we have been able to achieve in the 400 cm^2 cells is typical of commercial RFB offerings.

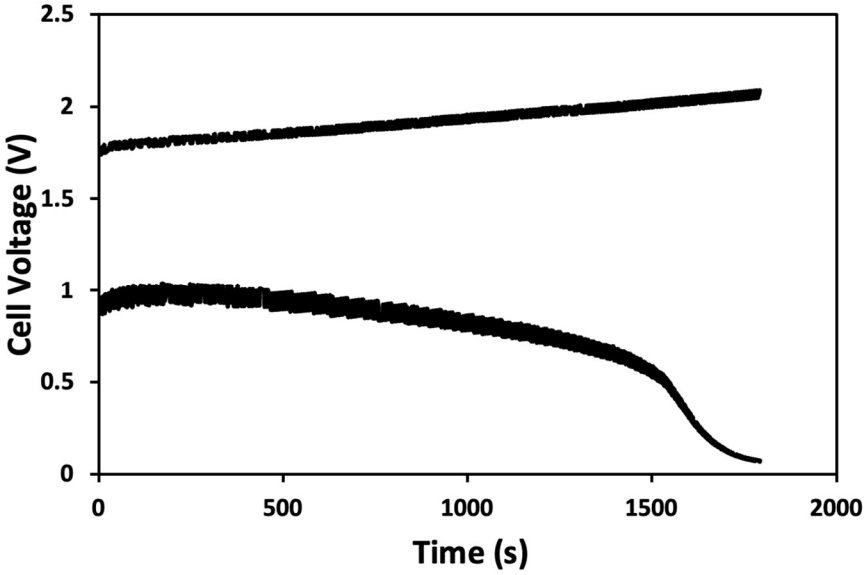

Figure 3.9 Representative charge-discharge curve of a Gen-1 H_2SO_4 based Ti-Ce RFB.

4. Results: Stack Testing (Summary of Work Performed at Giner Labs)

During this effort, Giner's focus was on scaling of the titanium-cerium electrode-decoupled redox flow battery system from the laboratory scale to a multi-cell short-stack modular design. Throughout the course of the effort, we designed a new test stand specifically for flow batteries, ensured component compatibility in a 5 cm^2 laboratory scale and ultimately managed to demonstrate brief cycling of a multi-cell stack.

4.1 Design of Flow Battery Test Stand

While Giner has 50 years of experience testing both electrolyzers and fuel cells at various scales, we did not have available hardware that was able to cycle a flow battery. Initially, the flow battery was tested on an electrolyzer test stand, but it was quickly realized that this was not able to provide the capabilities that we needed. To ensure that we were able to safely cycle the flow battery and collect necessary data, a test stand was designed consisting of both a power supply and load that could switch as the cell was charging and discharging. The hardware came with accompanying software which allowed for controlled charges and discharges with the ability to set voltage and current limits. This provided us a Giner the ability to program the desired cycling schedules. The test stand and software are shown in Figure 4.1.

Figure 4.1 a) Software used for controlling flow battery cycling and data acquisition and b) RFB test stand.

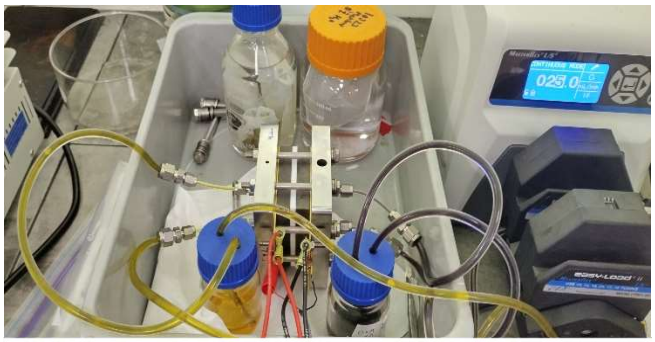

Figure 4.2 Photo of 5 cm^2 flow battery test setup

4.2 Laboratory Scale Testing

Initially, we had been working to integrate the Ti-Ce ED-RFB design from Washington

University directly into our 50 cm^2 modular/scalable stack as we looked to quickly achieve larger cell designs. While some initial cycling was achieved at this scale, we suffered from many issues due to high resistance which likely occurred from improper compression of the cell. These issues were evident as the cell quickly polarized and short cycles occurred often. To allow for rapid evaluation and remedy of these issues, we decided to briefly explore the RFB design within our 5 cm^2 lab scale hardware; this change allowed for decreased materials consumption as well. The 5 cm^2 cell build is shown in Figure 4.2 and consists of the AEM membrane sandwiched between two flow fields. A custom Teflon frame was machined in-house to allow for proper sealing of the analyte electrode while common gaskets were used for the catholyte side of the cell. With this cell architecture, we were quickly able to realize a leakless design, Figure 4.3, through several days of cycling.

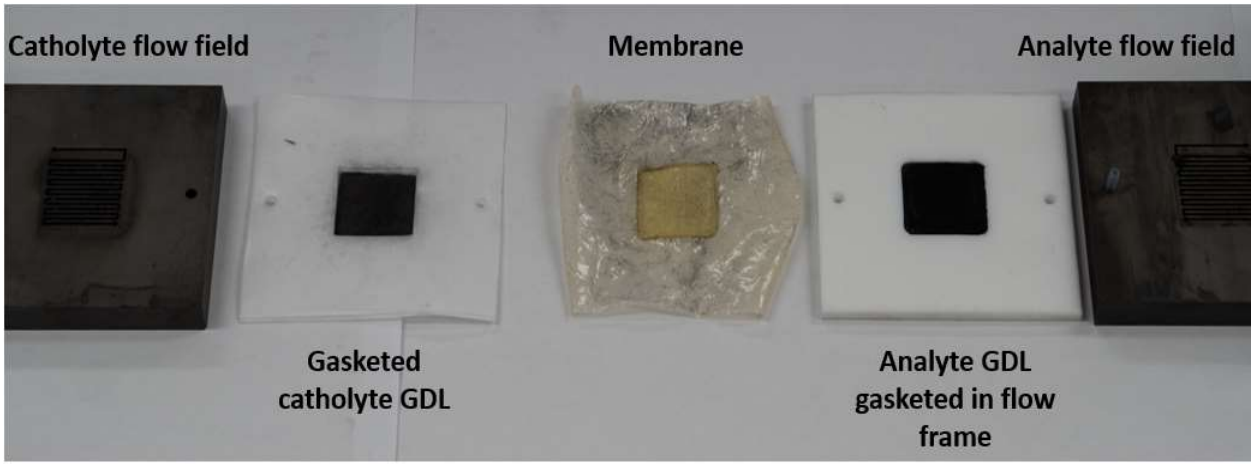

Figure 4.3 Overview of components used in 5 cm^2 electrolyzer testing; assembled set-up sandwiched between stainless steel endplates

Several successful 5 cm^2 cell runs were achieved during this phase of the project at various theoretical capacities. Prior to operation, carbon paper was activated at 500 °C for 8 hrs while bismuth electrodeposition was completed on the analyte GDL. Tests were carried out with 0.9 M Ce^+/4 M methanesulfonic acid (MSA) catholyte and 0.9 M Ti^+/4 M MSA analyte cycling at 100 mL/min and at room temperature. The protocol for charge discharge cycling was as follows: Galvanostatic charge at 100 mA/cm^2 to a cut off voltage of 1.85 V followed by potentiostatic charging at 1.85 V to 4 mA/cm^2. After a brief 5-minute pause, there was a Galvanostatic discharge at 100 mA/cm^2 until a lower limit voltage of 0.3 V was reached at which a potentiostatic discharge occurred until a current density of 4 mA/cm^2 was obtained. Another 5-minute pause occurred before the next cycle began. Cycling data for a cell with a theoretical capacity of 1 Ah is shown in

Figure 4.4a. For the first several cycles, round-trip, coulombic efficiency continuously increased before reaching a maximum efficiency of over 99% around the 7th cycle. While this did begin to decrease following that cycle, the performance provided promising data and evidence for improvements that could be made in our 50 cm^2 design. The cell also had discharge capacities at over 70% of the theoretical capacity until dropping off around cycle 7. The failure mechanism was further elucidated through the voltage profiles, Figure 4.4a. From these profiles, it can clearly be seen that the cell is polarizing during charging resulting in more efficient discharges than charges with the cut-off voltage for charging being reached very early into the charging process by cycle 8. Additionally, carbon paper was seen shedding into the catholyte which may be due to the geometry of this cell. From this work, we determined that there was a need for better compression on the thin, catholyte (cerium) part of the cell. This represented a departure from the commonly used components in Giner electrolyzer but certainly had a basis for design from previous R&D work.

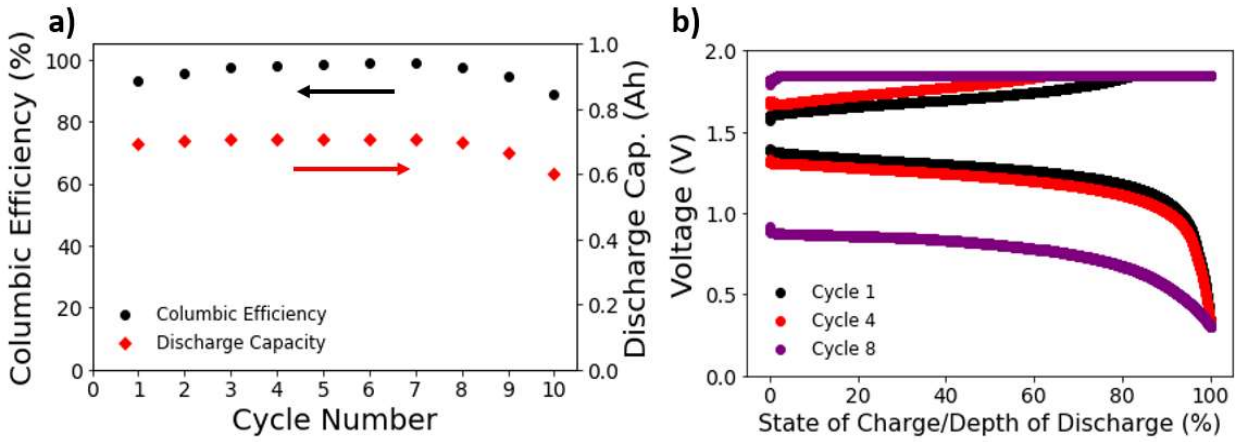

Figure 4.4 Experimental results for 5 cm^2 flow battery experiments with a) 1 Ah theoretical capacity, targeted 2-hour cycle duration and b) voltage profile of the same cell. 100 mL/min of flow with 0.9 M Ce^+/4 M MSA catholyte and 0.9 M Ti^+/4 M MSA analyte.

4.3 Single Cell Stack Testing

Testing beyond the lab scale was done at a 50 cm^2 cell active area with the intention of integrating this system with Giner's mass produced electrolyzer stacks. Due to the possibly corrosive nature of the 4 M methanesulfonic acid used to dissolve the electrolytes, it was critical to select compatible components when building. While Teflon was used at the smaller scale, this material is generally considered undesirable due to its flexibility and difficulty to machine to the thicknesses needed within the 50 cm^2 design. Ultimately, after thorough analysis, it was determined that flow

frames within the cell would be machine from Polyether ether ketone (PEEK) due to its excellent chemical resistance. Additionally, endplates were machined from stainless steel while current collectors were designed from titanium. The carefully machined PEEK flow frames are shown in Figure 4.5a&c while the completely assembled cell is shown in Figure 4.5b**.** As briefly mentioned in the previous section, one additional change that was made was the inclusion of a custom made, POCO graphite flow field, to fit our flow battery cell. This POCO flow field has a special coating to ensure improved conductivity and chemical resistance. This flow field, Figure 4.6, ultimately allowed for much improved liquid distribution within the active area.

For actual cell operation, a theoretical capacity of 10 Ah was targeted requiring 414 mL of electrolyte. Tests were carried out with 0.9 M Ce^{+}/4 M MSA catholyte and 0.9 M Ti^{+}/4 M MSA analyte cycling at 100 mL/min and at room temperature. Protocol was as with previous single cell experiments. These experiments initially showed successful cycling however, at this scale leaks were quickly noticed which ultimately led to poor efficiency and poor electrical connection throughout the cells. Through several more experiments we were able to gain a better grasp on the sealing requirements of the Ti-Ce ED-RFB. These improvements were then implemented as we made the upgrade to a short stack.

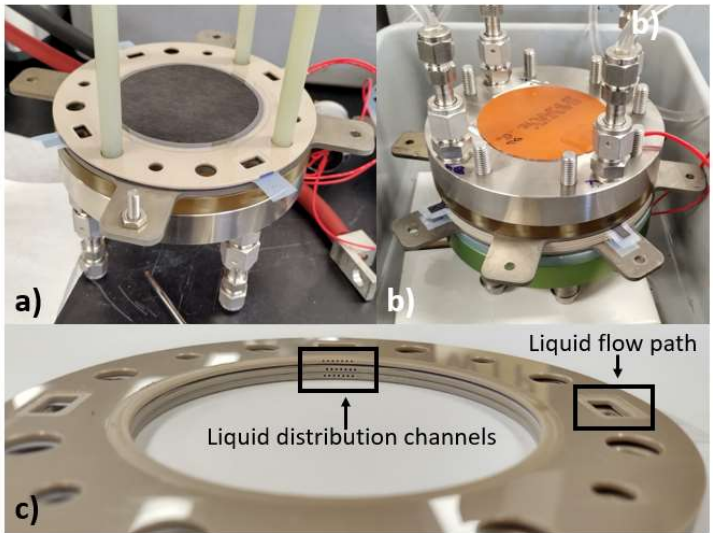

Figure 4.5. a) Carbon paper nested inside of PEEK flow frame, b) completely assembled single cell stack, and c) detailed image of the PEEK flow frames.

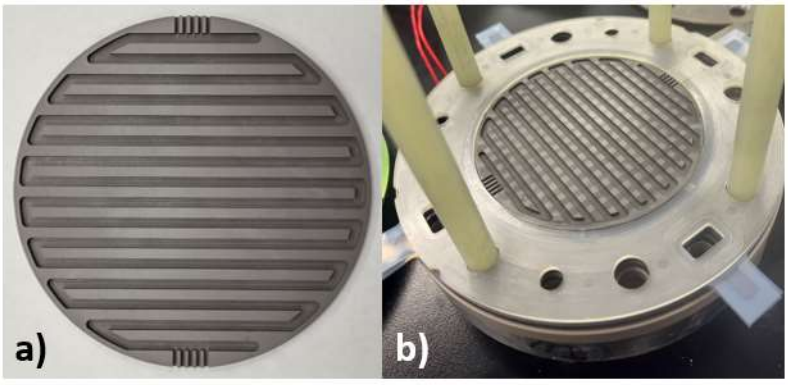

Figure 4.6. Custom machine POCO graphite flow field both a) alone and b) shown inside of a representative flow frame.

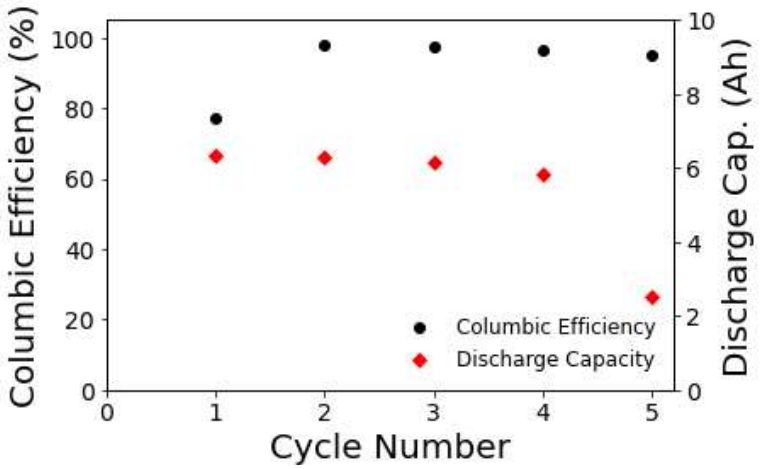

Figure 4.5 Experimental results for 50 cm² flow battery experiments with 10 Ah theoretical capacity, targeted 2-hour cycle duration. Operating conditions in text.

4.4 Short-Stack Testing

Short stack testing was done with a 3-cell stack as shown in Figure 4.6a**.** This cell was assembled in a monopolar fashion such that total current was increased with each cell, resulting in a charge/discharge current of 15 A for the 3-cell stack. A clear demonstration of the configuration is shown in Figure 4.6b**.** The stack was assembled with internal flow fields and components like the single cell design. Operating conditions were scaled such that 2-hour cycles were targeted (30 Ah). Cycling consisted of the same solutions, voltages and current densities as the single-cell stack, but electrolyte flow was increased to 300 mL to account for the increased area.

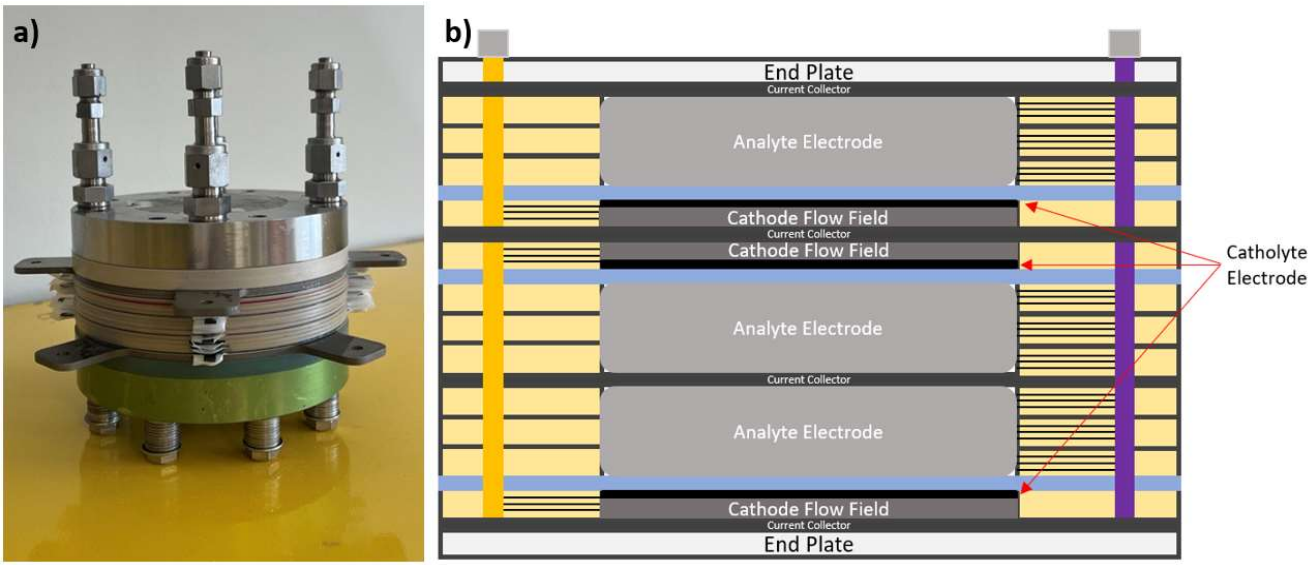

Figure 4.6. a) Assembled 3-cell, 50 cm² Ti-Ce ED-RFB stack and b) schematic of cell internals showing monopolar cell construction. Gaskets are omitted for clarity.

Due to time constraints, only several cycles were run during this effort. While columbic efficiency, Figure 4.7a, remained over 98% for the cycles that were run, due to the polarization on charge that can be seen in Figure 4.7b, the energy efficiency held around 50% as opposed to the desired 60+%. Nonetheless, the voltage profiles show clear room for further improvement and the possibility for extended future operation. One major improvement as we moved to the 3-cell stack was that improved sealing was seen for the system. With the leaking issues that had been seen with the previous stack no longer apparent despite the duration of cycling and the high electrolyte flow rate (300 mL/min) being forced through the cell. This likely contributed to the more stable round-trip columbic efficiencies compared to that which had been seen previously. Future stacks consisting of more cells would provide similar results.

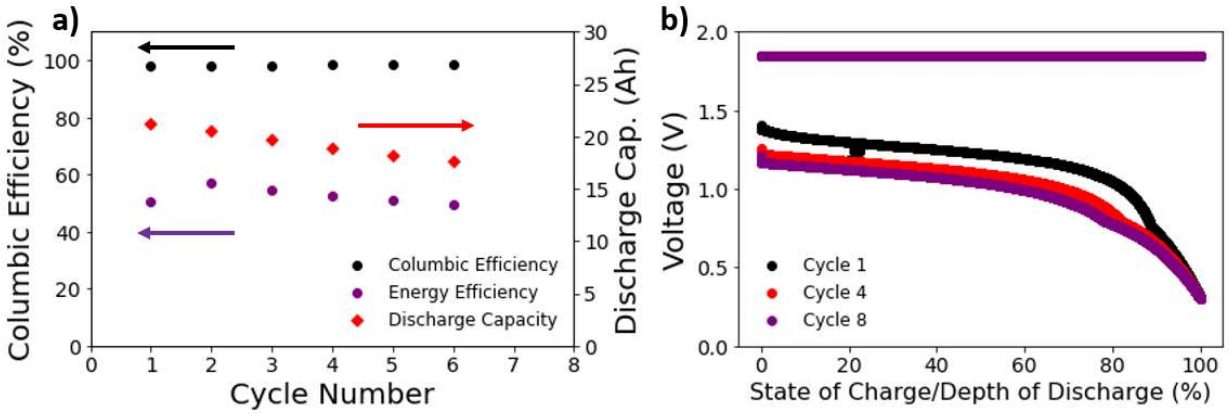

Figure 4.7 Cycling data for the 3-cell short-stack. Including a) columbic efficiency, energy efficiency, and discharge capacity, and b) voltage profiles. Conditions mentioned in text.

Future considerations

As we look to further scale-up, the final experiments completed at Giner show certain promise for the future. Results from the 3-cell short stack show that with further optimization of cell compression and components will lead to successful operation of the Ti-Ce ED-RFB over longer duration at the multi-cell stack level. While results from the experiments still show issues with polarization and some leaking, these are certainly improvable with further efforts.

5. List of Products Resulting from Project

Peer-Reviewed Journal Publications:

S. Ahmed, M. Shahid, S. Sankarasubramanian, Aqueous Titanium Redox Flow Batteries - State-of-the-art and Future Potential, *Frontiers in Energy Research* (2022) DOI: 10.3389/fenrg.2022.1021201.

Conference Presentations & Proceedings:

S. Ahmed, S. Sankarasubramanian, Electrochemical and Spectroscopic Investigation of Solvation and Complexation Effects on Titanium Redox Flow Battery Electrolytes, 243nd ECS meeting, Boston, MA (May 28, 2023 - June 2, 2023).

S. Ahmed, D. Torres, M. Shahid, S. Sankarasubramanian, Tailoring Solvation and Counterion Complexation in the Electrolyte for Enhanced Titanium Redox Flow Battery Performance, 242nd ECS meeting, Atlanta, GA (October 9-13, 2022)

Kumfer, B., *Titanium-Cerium Electrode-Decoupled Redox Flow Batteries Integrated with Fossil Fuel Assets for Load-Following, Long-Duration Energy Storage*. presented at the NETL Advanced Energy Storage Initiative Program Project Review Meeting (Virtual) April 5-6, 2021.

Kumfer, B., Sankarasubramanian, S. *Titanium-Cerium Electrode-Decoupled Redox Flow Batteries Integrated with Fossil Fuel Assets for Load-Following, Long-Duration Energy Storage*. presented at the NETL Advanced Energy Storage Initiative Program Project Review Meeting (Virtual) May 5, 2022.

Kumfer, B., *Titanium-Cerium Electrode-Decoupled Redox Flow Batteries Integrated with Fossil Fuel Assets for Load-Following, Long-Duration Energy Storage*. presented at the NETL FECM Annual Meeting in Pittsburgh, PA, April 18-20.

6. References

1 Eser, P., Singh, A., Chokani, N. & Abhari, R. S. Effect of increased renewables generation on operation of thermal power plants. *Applied Energy* **164**, 723-732, doi:https://doi.org/10.1016/j.apenergy.2015.12.017 (2016).

2 Holttinen, H. *et al.* in *Conference: Presented at the 10th International Workshop on Large-Scale Integration of Wind Power into Power Systems as well as on Transmission Networks for Offshore Wind Power Plants, 25-26 October 2011, Aarhus, Denmark* Medium: X; Size: 6 pp. (Langen, Germany: Energynautics GmbH, United States, 2011).

3 Hong, L., Lund, H. & Möller, B. The importance of flexible power plant operation for Jiangsu's wind integration. *Energy* **41**, 499-507, doi:https://doi.org/10.1016/j.energy.2012.02.038 (2012).

4 Keatley, P., Shibli, A. & Hewitt, N. J. Estimating power plant start costs in cyclic operation. *Applied Energy* **111**, 550-557, doi:https://doi.org/10.1016/j.apenergy.2013.05.033 (2013).

5 Descriptions of Past Research: Impacts of Cycling on Existing and Future Fossil Assets. Report No. 3002012469, (Electric Power Reserach Institute, Palo Alto, CA, 2017).

6 Power Plant Cycling Costs. Report No. NREL/SR-5500-55433, (National Renewable Energy Laboratory, 2012).

7 Annual Energy Outloook. (US Energy Information Administration https://www.eia.gov/outlooks/aeo/, 2023).

Appendix 1. Technology Maturation Plan (TMP)

Current TRL level	4
End-of-project TRL level	4-5

The titanium-cerium electrode-decoupled redox flow battery (Ti-Ce ED-RFB) has been developed to a TRL level of 4 ("component and/or system validation in laboratory environment") over the course of a prior project funded by ARPA-E. We have prepared Ti and Ce electrolytes and used them in an ED-RFB configuration using off-the-shelf, plate-and-frame type single electrochemical cell hardware (**Fig. 1**) and custom anion exchange membranes. In the prior project, our full-cell tests at the 25 cm^2 single-cell scale have yielded over 1300 hours of continuous cycling with no loss in normalized capacity with > 60% energy efficiency, thereby demonstrating its long-term durability (**Fig. 2**). Further, the RFB was charged to 90% of its maximum capacity, the electrolytes were withdrawn to the storage tanks and allowed to stand for 4 days (96 hours) followed by pumping the electrolyte back into the cell and discharging it. No changes in the polarization behavior were observed and the unchanged open circuit voltage indicated that state-of-charge (SOC) was unchanged (**Fig. 3**). This experiment demonstrated the claimed long-duration stand-by capabilities of this ED-RFB. Thus, having demonstrated the continuous operation of these cells in a laboratory setting, we have met all aspects of the TRL 4 designation

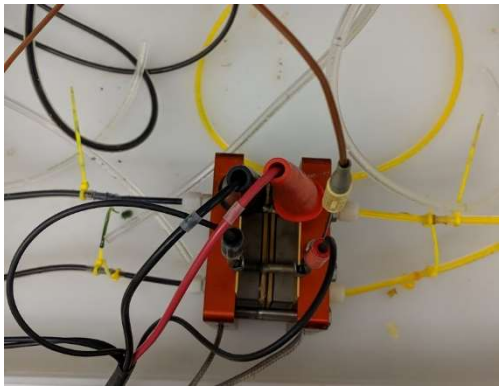

Fig 1. Top-view of the Ti-CE RFB with a QPEK-C separator and methanesulfonate counterion.

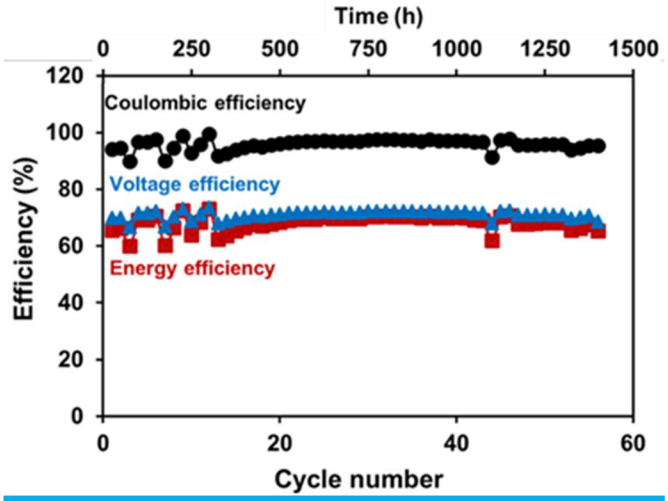

Fig. 2 Long-term cycling efficiencies of a Ti-Ce ED-RFB.

that *"The basic technological components are integrated to establish that the pieces will work together."*

The Ti-Ce ED-RFB technology benefits greatly from the decoupling of energy output and power output inherent in RFBs. Thus, the system can be suitably scaled to meet diverse operational requirements. Target commercial applications are energy storage over - **1)** short duration (< 1 hour to hourly) for ***voltage and frequency support and spinning reserve reduction/elimination***; **2)** intermediate duration (multi-hour to full-day) for ***peak load demand and arbitrage opportunities*** considering diurnal load profiles and weather forecasting; **3)** long duration (multi-day) to improve system resiliency against prolonged interruptions and to capture large amounts of energy during periods of high renewables penetrations / low demand. Over the course of the project, we will determine the most utility relevant application based on feedback from our partner Ameren Missouri and design the system for that specific application. Assessment of Ti-Ce ED-RFB integration with specific existing power plant assets of Ameren may also be carried out to refine the commercial application specifications.

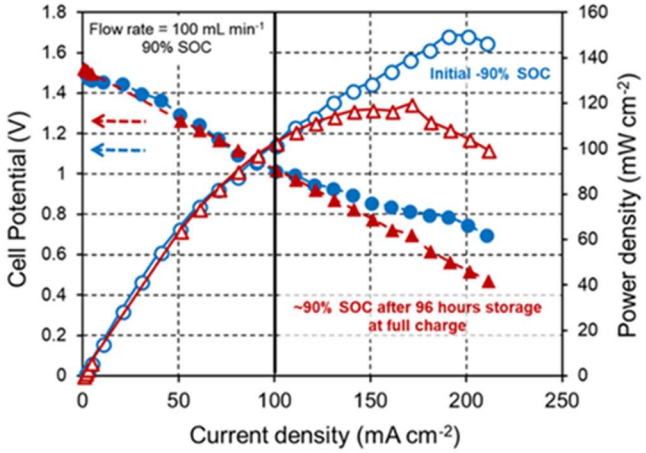

Fig. 3 Demonstration of 96h stand-by at 90% state of charge (SOC) condition.

B. PROPOSED WORK

The project is designed to be executed as a series of Ti-Ce ED-RFB size and performance scale-up steps informed by market and techno-economic analyses and input from our fossil fuel asset partner Ameren Missouri. The table below summarizes the various stages of the project -

Project stage	Present	Intermediate	Final
Representative cell/stack images	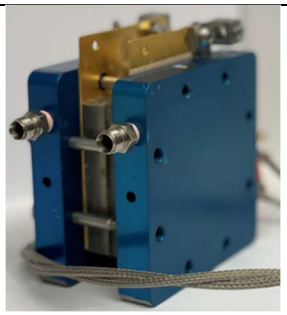		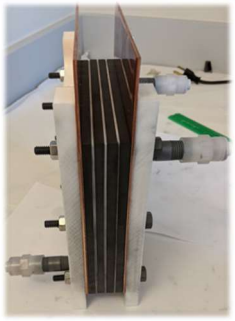
TRL level	4	4-5	5
# of cells	1	1	Up to 10
Area per cell (cm^2)	25	400	400
Current density (mA/cm^2)	100	200	200 (can be modified based on TEA)
Avg. discharge voltage (V)	1	1.2	1.2
Power density (mW/cm^2)	100	240	240
Total Power (W)	2.5	96	Up to 960
Discharge duration	Up to 24-h (limited only by electrolyte volume)	Up to 48-h (limited only by electrolyte volume)	Up to 48-h (limited only by electrolyte volume)
Energy efficiency (%)	≥50%	≥60%	≥60%
Notes	Demonstrated capability to stand-by for 4 days		

Over the course of the project, the project team aims to scale-up the current 25cm^2 cell initially to larger cell sizes (400cm^2, 16x scale-up) and subsequently to short-stack levels (3-5-10 cell stack, 400 cm^2 cells, ultimate 160x scale-up). This will be done in cooperation with Giner Inc. (subcontractor) In addition to standard charge-discharge cycles of equal duration we will also evaluate load following performance by - **(i)** asymmetric cycling (charge and discharge at different current densities), **(ii)** incomplete cycling (e.g., charge to 60% SOC and discharge) and **(iii)** discharge following extended storage of charged (or partially charged) actives. The design and performance attributes of this RFB cannot directly be compared to current near-commercial systems like the all-vanadium RFB due to the novel electrolyte chemistry and the different separator operational mechanism (anion exchange membranes (AEMs) as opposed to cation exchange membranes (CEMs)). Thus, we have defined the power density based on the preliminary cost analysis presented in **Fig. 4**. We found that increasing the power density to 1.5-2.0 kW/m^2 (per cell) led to a significant drop in the power components cost which plateaus off at higher power densities. Thus, 2.0 kW/m^2 was chosen as our target (200 mA/cm^2 @ 1V). All-V RFBs operate at higher power densities (potentially leading to accelerated graphitic flow field damage) to offset their much higher energy component (i.e., electrolyte) costs. The efficiency targets were also obtained from this preliminary modeling result where we identified pathways to meet the DOE cost target of $100/kWh for RFBs, which corresponds to the approximate limit for Li-ion cells[1]. The duration is specified based on anticipated diurnal and multi-day load profiles. We anticipate modifying this duration following a forecasting analysis with our utility partner Ameren Missouri.

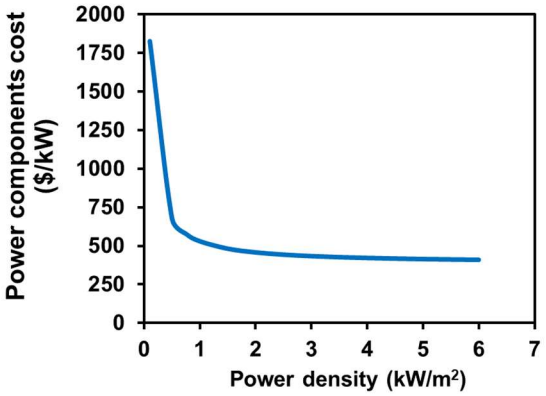

Fig 4. RFB stack power components cost as a function of stack power density.

Equipment/test system requirements: The team has access to extensive testing hardware at both WUSTL and at Giner. The team also has access to several machine shops for fabrication of the components of the RFB cells and stacks. The team has in-house membrane coating facilities that allow the manufacture of up to 20cm wide membrane rolls for the RFB separator. We have also identified 2 contract manufacturers who can fabricate even wider membranes if needed over the course of the project. Additionally, large RFB stack testing units will be shortly commissioned

through Ramani's ONR DURIP grant and will be housed in Ramani-led WashU Energy Center (a newly renovated additional 3000 sq. ft. of lab space). Apart from scaled-up cell and stack fabrication, we do not currently anticipate the need for any new testing equipment,

Final TRL level and justification: The final project TRL will be 5. The stacks that will be designed and fabricated over the course of Subtask 2.3 and 2.4 will be representative, almost-prototypical RFB modules. Any future deployment of RFBs will involve *n* number of these units connected together as per requirement and hence this unit (made as part of the project) would represent a first-of-its-kind, engineering-scale Ti-Ce RFB model. Thus, this would meet the TRL 5 criteria of "The basic technological components are integrated so that the system configuration is similar to (matches) the final application in almost all respects." The cells will be tested under various charge/discharge scenarios to achieve a simulated application environment. The capacity of the final stack will approach the kW scale, which is a maximum for a lab-scale system. For application in the utility power generation sector, an increase of 1 to 2 orders of magnitude would be needed for a pilot-scale demonstration (TRL 6). Furthermore, through execution of a preliminary engineering design and techno-economic analysis of a utility-scale fossil power plant with an integrated RFB system, we will make progress towards achieving TRL 6 criteria of "Engineering-scale models or prototypes are tested in a relevant environment." The design created as part of subtask 2.3 will yield scaling factors and dimensionless parameters that will enable the eventual transition from TRL 5 to TRL 6 by allowing "….the determination of scaling factors that will enable design of the operating system"

C. POST-PROJECT PLANS

The further development of this system at higher TRL would involve the engineering scale-up of the stack developed in this project. This will be carried out using the scaling factors and relationships identified in this project. Given the engineering nature of this next stage, we anticipate that it would be more suitable for a commercial entity specializing in this area (possibly Giner Inc). The project ends with the development a first-of-its-kind stack, providing the know-how for the commercial manufacture of the next *n* units. Thus, this is the ideal end point for the project.

References:

1. US DOE, ARPA-E FOA 0001478 "INTEGRATION AND OPTIMIZATION OF NOVEL ION CONDUCTING SOLIDS (IONICS)" (2016). https://arpa-e-foa.energy.gov/Default.aspx?foaId=d3b62d65-4754-4cb4-b879-d2e6cea654eb

2.http://www.mckinsey.com/business-functions/sustainability-and-resource-productivity/our-insights/the-new-economics-of-energy-storage;

3.https://www.luxresearchinc.com/hubfs/Lux%20Research%20-%20Global%20Energy%20Storage%20Market%20Forecast%202019%20-%20press.pdf

Appendix 2. Commercialization Plan

Market assessment: The stationary energy storage market in the US has been growing at a higher than projected cumulative annual growth rate (CAGR) over the past 5-years. The market is predicted to triple over the next 5 years (**Fig. 1** created from references 2 and 3, Appendix 1).

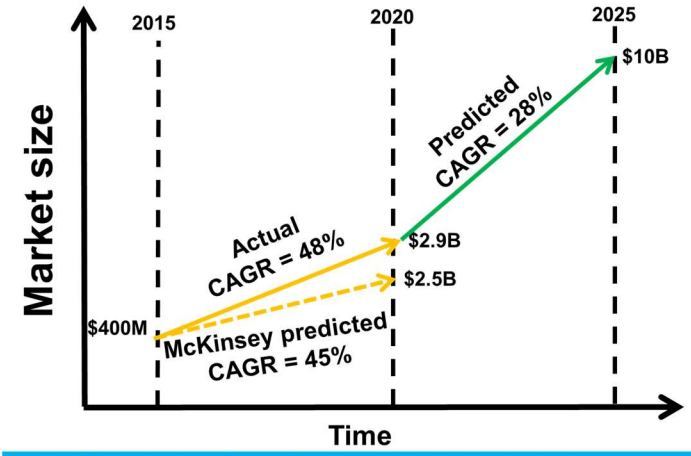

Fig 1. The US stationary energy storage market projections.

Technology commercialization vehicle: Presently, we anticipate demonstrating the Ti-Ce RFB as a cost-effective energy storage solution for the electric grid and hence developing licensing interest in this technology. The team has received a patent on the enabling AEM technology (US 10,910,656 B2) and has another pending on the Ti-Ce RFB (US 2019/0280323 A1). The team is actively engaged with the Office of Technology Management at WashU to develop licensing opportunities. Based on anticipated commercial interest, we may also elect to develop this technology through a suitable start-up vehicle.

Appendix 3. Technology Gap Assessment

During the execution of the project, two key technical hurdles were experienced that should be focal points of future R&D efforts. It was found that the square-cell Ti-Ce system developed by WashU was not so easily adaptable to other existing electrochemical test platforms. Third-party validation required a substantial retrofit of the teaming partner's existing test cells to accommodate alternative membrane, gasket, and flow field materials. Ultimately, these alternative materials were successfully acquired and deployed after some trial and error. However, these extensive retrofitting activities prevented direct scale up to a multi-stack, 1 kW system. In parallel, the WashU test cell design was directly scaled-up by UTSA to 400 cm^2, but challenges also arose with system sealing that prevented long-term operation. To fully advance to TRL 5, the team should seek to partner with an RFB cell technology developer with experience and proven hardware at the 1 kW scale that is more readily adaptable to the Ti-Ce system. Future R&D should focus heavily on large-scale cell/stack design and investigate opportunities to reduce cost through alternative stack materials and configurations.

The second technical gap pertains to the electrolyte stability and formulation. The team experienced difficulties in obtaining Ce precursor chemicals of sufficient purity, noting that actual purities sometimes differed from what was indicated by the vendors. Impurities were found to lead to unwanted precipitation of solids which restricted the electrolyte molarity. UTSA is continuing to investigate alternative Ce electrolyte formulations and complexation effects to improve the stability at high molarity. It is recognized that some limited crossover of metals through the membrane may occur over time, thereby contaminating the electrolytes and degrading cell performance. This is expected to be easily remedied through a routine maintenance procedure whereby the pH is adjusted to cause selective precipitation of the unwanted metal. This procedure should be demonstrated and optimized in future R&D work.

Appendix 4. TEA Initial Design Basis

1 CASE DESCRIPTIONS

1.1 Power Plants

A total of four fossil power plants are considered. Two of the plants are hypothetical reference plants described in the NETL Report: *Cost And Performance Baseline For Fossil Energy Plants Volume 1: Bituminous Coal And Natural Gas To Electricity*, which was most recently updated in 2019 [1]. The other two cases represent an actual operating natural gas-fired power plant. At present, the plant consists only of simple-cycle combustion turbines. A retrofit to include a combined steam cycle will also be considered. An overview of each plant site is given below. Detailed component and site specifications are outlined in subsequent sections.

1. Reference NGCC (NETL Baseline Case 31A)

The design is based on a market-ready technology that is assumed to be commercially available at the time the project commences. Each design consists of two state-of-the-art 2017 F-class combustion turbine generators (CTGs), two heat recovery steam generators (HRSGs), and one steam turbine generator (STG) in a multi-shaft 2x2x1 configuration. The Rankine cycle portion uses a single reheat 16.5 MPa/585°C/585°C (2,393 psig/1,085°F/1,085°F) subcritical steam cycle. This hypothetical plant is located at a reference site in the Midwest.

2. Reference NGCC w/ CDR (NETL Baseline Case 31B)

The design is the same as above reference plant, but with the addition of a carbon dioxide recovery (CDR) facility. The CDR is designed to remove 90 percent of the CO_2 in the flue gas exiting the HRSG, purify it, and compress it to a supercritical condition. The CDR comprises flue gas supply, CO_2 absorption, solvent stripping and reclaiming, and CO_2 compression and drying. The CO_2 absorption/stripping/solvent reclamation process is based on the Cansolv system.

3. Venice Energy Center CT (simple cycle)

The Venice Energy Center (VEC) is an existing natural gas fired “peaking” power plant owned and operated by Ameren and located in Venice, IL (just across Mississippi River from St. Louis, MO). The plant has a total of four CTGs; this study will focus on the two largest and newest F-class turbines (Siemens-Westinghouse 501F-D2).

4. Venice Energy Center NGCC

This plant design considers an upgrade of the above VEC plant to add two HRSGs and associated flue gas cleaning equipment for combined cycle operation. Information on the upgrade design will be taken from a prior engineering study commissioned by Ameren. The two HRSGs will drive a single STG. The Rankine cycle portion uses a single reheat 2,000 psia/1,050°F/1,050°F subcritical steam cycle.

1.2 Storage Implementation Scenarios

For each of the four power plant cases the size of an RFB storage system, both in terms of power (kW) and total energy (kWhr), will be determined based on several scenarios as described below. Each scenario is designed to achieve a different storage objective. In each scenario, it is assumed that the added generation capacity of the RFB is offset by reducing the output of a sister fossil plant such that the total, regional generation is unchanged.

Scenario A: No Storage

This scenario assumes a projected cyclic power plant load profile in the year 2030, in the absence of any energy storge integration. The load profile is described in more detail in Section 3 and is derived assuming that a regional load profile is to be met by mix of generation sources, including significant portions of intermittent wind and solar, resulting in deep cycling and fast ramp rates for the fossil fleet. This plant load profile is considered as a reference baseline for the other scenarios below.

Scenario B: Short Duration (0-2 hours)

In this scenario, a "peaker" RFB storage system is designed to discharge for up to 2 hours during hours of peak demand, and charge during off-peak hours. The objective of this scenario is to maximize value and revenues through arbitrage and the avoidance of market purchases during times of high electricity demand, and by limiting the size of the RFB system to reduce the capital costs, as compared to other cases.

Scenario C: Intermediate Duration (2-24 hours)

In this scenario, an RFB system is added with sufficient generation capacity such that the dynamic cycling feature of a daily load profile will be fully met by the RFB while the fossil power plant operates steadily at maximum capacity factor, to maximize the efficiency of the fossil plant and minimize costs due to cycling.

Scenario D: Long Duration (24-48 hours)

In this scenario, an RFB system is added with ample storage and power capacity for multi-day (48-hour) cycling. The objective of this scenario is to improve system reliability by creating a generation asset that may be dispatched continuously for days during periods of unexpected system outages or severe or unusual weather events.

A summary of the cases with the case identifiers is listed below in Table 2.1

Table 1.1 TEA Case Identifiers

Fossil Plant	Scenario A: No Storage	Scenario B: Short Duration	Scenario C: Intermediate Duration	Scenario D: Long Duration
1. Reference NGCC NETL Baseline Case 31A	1A	1B	1C	1D
2. Reference NGCC w/CDR NETL Baseline Case 31B	2A	2B	2C	2D
3 VEC CT (simple cycle)	3A	3B	3C	3D
4. VEC NGCC	4A	4B	4C	4D

2. LOAD CASES

U.S. DOE envisions that the U.S. will be a world leader in energy storage utilization and exports by the year 2030 [2]. The Ti-Ce ED-RFB technology is also on a path to be commercially available by that time. A projected 2030 regional load and generation profile is therefore developed that assumes substantial increased deployment of renewable sources as compared to today. The regional load profiles shown below were developed using data from a prior Monte-Carlo study commissioned by a midwest electric utility company that currently owns and operates over 10,000 MWe of generation capacity. These reference profiles assume zero energy storage capacity and are treated as a baseline (Scenario A) such that the costs and benefits of adding storage can be assessed. The generation is broken down by source type (nuclear, wind, solar, fossil). The baseline fossil generation profiles will be modified to reflect addition of storage for Scenarios B-D as an outcome of this study.

Baseline projected weekly load profiles for this hypothetical fleet are shown in Figures 3.1(a-c), which correspond to representative weeks in the Winter, Spring, and Summer seasons, respectively. This fleet consists of 600 MW of solar and 1200 MW of wind (nameplate) capacity, and 1200 MW of baseline nuclear. In this scenario the instantaneous share of total renewable generation is projected to reach 35% in the Spring season when overall demand is lowest.

A baseline, seasonal weekly generation profile for each power plant (reference NGCC and VEC plants) is derived by rescaling the fossil fleet generation profiles. This effectively assumes that each fossil plant in the fleet follows the same ramping profile. Normalized profiles are shown in Fig. 3.1(d-f), and the actual plant profile is derived by multiplying by the plant generation capacity. The resulting plant load profiles indicate deep cycling in the spring and high ramp rates in all seasons that are challenging for steam-generating fossil sources to achieve. It is recognized that existing peaking combustion turbines and pumped-hydro facilities will reduce the cycling burden on steam-generating units to some extent. Nonetheless, for the purposes of this study, extreme cycling of steam-generating units should be anticipated in light of aggressive renewable energy targets and potential increasing variability in weather patterns.

It is noted that, particularly in the spring season, daily sharp spikes in fossil generation can result due to the misalignment of peak demand with peak solar generation and the coincident falloff of solar generation with the rising demand. These spikes highlight a potential case for short-term battery capacity addition (Scenario B).

Regional generation by source | Normalized fossil generation

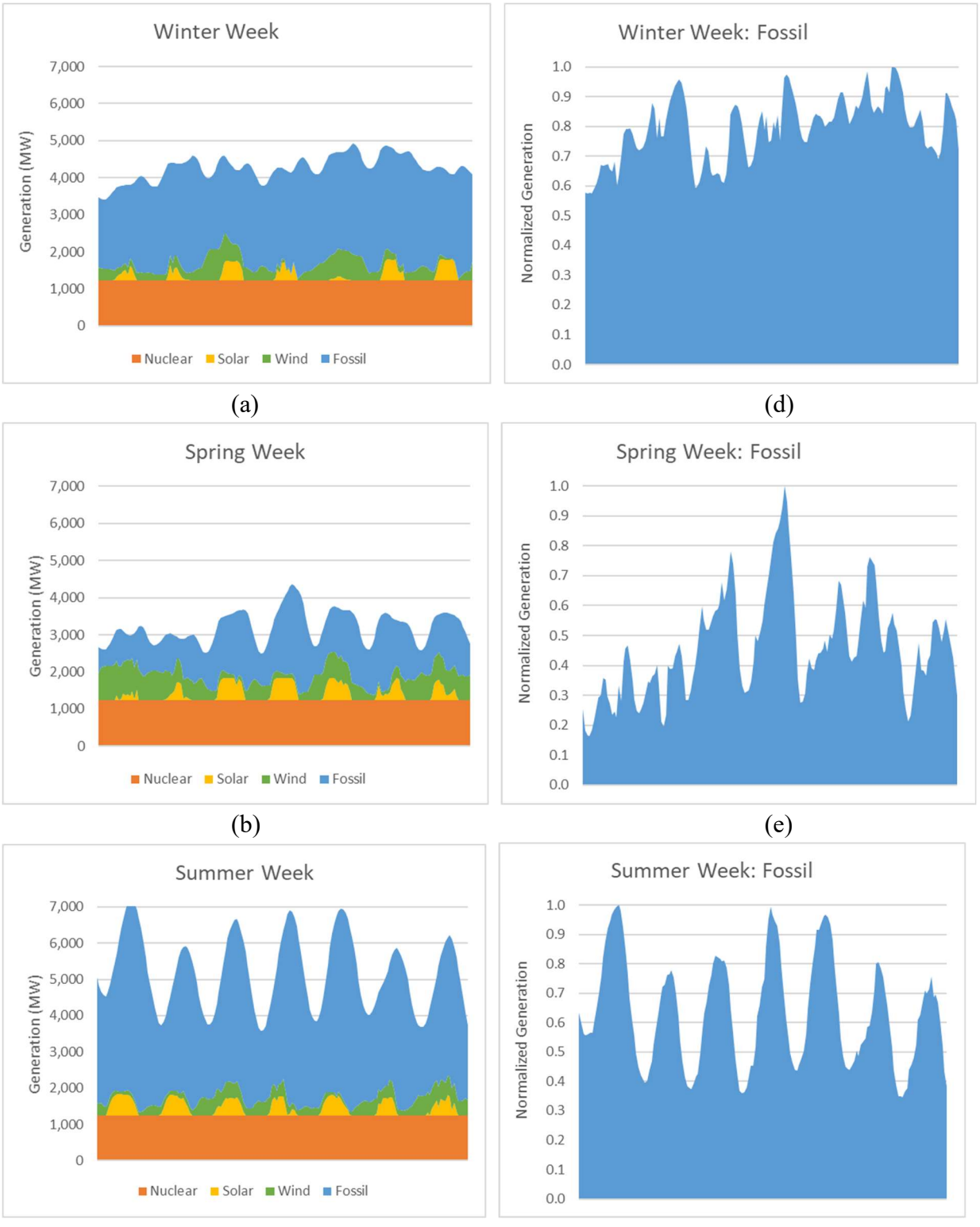

Fig. 2.1 – Seasonal, weekly generation profiles projected for the year 2030. (a)-(c): regional generation profiles broken down by source. (d)-(f): normalized fossil plant generation profiles

3. GENERAL CRITERIA AND PHILOSOPHY

3.1 Sparing Philosophy

Normal sparing of critical rotating equipment shall be included, such as feedwater pumps, condensate pumps, circulating water pumps, and electrolyte pumps. Where equipment size considerations may force multiple trains, multiple train equipment will be reviewed on a case-by-case basis based on operations at part load for sparing requirements.

3.2 Effects of Plant Cycling on Maintenance and Efficiency

The costs associated with operating the power plant under cyclic conditions with high ramp rates are to be quantified. Operating the plant a lower load reduces the plant efficiency, thereby increasing fuel costs and emissions, due to losses associated with valve/damper throttling, operating pumps and fans at non-design conditions, and steam attempering. The plant efficiency as a function of load will be calculated through ASPEN process modeling and literature review of prior studies. Routine maintenance costs associated with replacement of high-temperature turbine blades and combustor components will be included and calculated as a function of the number of effective starts, ramp cycle frequency, and total operating hours. Frequent cycling is also anticipated to increase thermal fatigue on steam components, leading to an overall increase in maintenance and repairs. These impacts from cycling will be estimated based on anecdotal evidence from plant operators and literature survey.

3.3 Plant Personnel

It is assumed that the battery storage system will require one full-time operator, that is in addition to power plant staff. Maintenance will be performed by contractors external to the plant.

3.4 General

The following design parameters are considered site-specific and are not quantified for this study. Allowances for normal conditions and construction are included in the cost estimates:

- Flood plain considerations
- Existing soil/site conditions
- Water discharges and reuse
- Rainfall/snowfall criteria
- Seismic design
- Buildings/enclosures
- Fire protection
- Local code height requirements
- Noise regulations (impact on site and surrounding area)

Decommissioning processes and costs are also excluded.

4. SITE CHARACTERISTICS

Two sites will be evaluated in this study: a generic Midwestern U.S. plant site, and the Venice Energy Center in Venice, IL. The site characteristics and ambient conditions for each are presented in Table 5-1 and Table 5-2. The ambient conditions for Cases 1 & 2 are the same as those listed in the NETL Cost and Performance Baseline for Fossil Energy Plants. A satellite view of the twin combustion turbines at VEC is shown in Fig. 5-1, with space available to the south for battery storage and for the HRSG and cooling towers for Case 4.

Table 4-1 Site Characteristics

Site Characteristics	Ref. NGCC (Cases 1 & 2)	VEC (Cases 3 & 4)
Location	Greenfield, Midwest	Venice, IL
Topography	Level	
Size (acres)	100	10
Transportation	Rail or Highway	
Cooling Water	50% Municipal and 50% Ground water	Case 3 (once through): Mississippi River Case 4 (tower): Ground water for makeup

Table 4-2 Site Ambient Conditions

Site Conditions	Ref. NGCC (Cases 1 & 2)	VEC (Cases 3 & 4)
Elevation, m (ft)	0 (0)	128 (420)
Barometric Pressure, MPa (psia)	0.101 (14.7)	
Design Ambient Dry Bulb Temperature, °C (°F)	15 (59)	
Design Ambient Wet Bulb Temperature, °C (°F)	10.8 (51.5)	
Design Ambient Relative Humidity, %	60	
Cooling Water Temperature, °C (°F)	15.6 (60)	
Air Composition, mass%		
H_2O	0.616	
AR	1.280	
CO_2	0.050	
O_2	22.998	
N_2	75.055	
Total	100.00	

Figure 4-1. Satellite view of the Venice Energy Center

5. FUEL SPECIFICATIONS

It is assumed that a natural gas main with adequate capacity is near to the site fence line (within 16 km [10 mi]) and that a suitable right-of-way is available to install a branch line to the site. It is also assumed that the gas will be delivered to the plant custody transfer point at sufficient pressure such that natural gas is available at the turbine inlet at 2.9 MPa (415 psig) and 27°C (80°F), which matches the state-of-the-art 2017 F-class fuel system requirements. Hence, neither a pressure reducing station, nor a fuel booster compressor is required. It is assumed that the natural gas has an added mercaptan composition of 5.75x10-6 mol%.

Component		Volume Percentage	
Methane	CH_4	93.1	
Ethane	C_2H_6	3.2	
Propane	C_3H_8	0.7	
n-Butane	C_4H_{10}	0.4	
Carbon Dioxide	CO_2	1.0	
Nitrogen	N_2	1.6	
Methanethiol	CH_4S	$5.75x10^{-6}$	
	Total	100.0	
	LHV		HHV
kJ/kg (Btu/lb)	47,201 (20,293)		52,295 (22,483)
MJ/scm (Btu/scf)	34.52 (927)		38.25 (1,027)

6. POWER PLANT BASELINE PERFORMANCE

Summary of Key Parameters

Parameter	Ref. NGCC		VEC	
	Case 1	Case 2	Case 3	Case 4
Combust. Turbine gross output (MWe)	2 x 238		2 x 169	
HRSG Steam Cycle (psig/°F/°F)	2,393/1,085/1,085		N/A	1772/1050/1050
Steam Turbine Power (MWe)	263	213	N/A	185
CO_2 recovery load (MWe)	N/A	28	N/A	
Bal. of Plant Loads (MWe)	14	16	18	19
Plant Gross (MW)	740	690	338	523
Plant Net (MW)	727	646	320	504
LHV Plant Efficiency (%)	59.4	52.8	35.9	53.6
LHV Heat Rate (Btu/kWh)	5,743	6,462	9,493	6,363
LHV CT Efficiency (%)	39.0		35.9	
NOx Control	LNB & SCR		LNB	LNB & SCR
CT Turbine Specifications				
Type	F-Frame		F-Frame (501F-D2)	
Outlet Temperature (°F)	1,156		1,116	
Plant Turndown Min Load (%)	22.0	N/A	50.0	22.0
Ramp Rate (MW/min)	80.0	N/A	tbd	tbd
Startup Time, RR Hot (min)	25	> 25	tbd	tbd
Electrical Specifications				
Grid Interconnect (kV)	345		138	

7. MAJOR COMPONENTS OF BATTERY SYSTEM

Component	Description/Notes
Cell Stack	
Membrane	QPEK-C-TMA-CI, produced in large rolls by Eastman Kodak
Bipolar plates	Composite material
Electrodes	Carbon felt
Current collectors	Copper with corrosion-resistant coating
Endplates and hardware	
Electrolyte	
Ti solute	
Ce solute	
Solvent	Sulfuric (~3-4 M) or methanesulfonic acid (~2M)
Mechanical/Misc	
Storage Tanks	Rated for sulfuric
Heat Exchanger	Plate & frame
Electrolyte pumps	Electric motor driven with variable speed drives
Isolation Valves	Compatible with electrolyte, motor driven
Housing	Shipping container to house stacks and critical components
Electrical for Grid Integration	
Inverter/Charger	
Step-up Transformers	
HV switches and breakers	
Racks/cables	
SCADA system	Fully-automated controls, data acquisition, HMI

8. BATTERY ENERGY STORAGE SYSTEMS PERFORMANCE MODEL

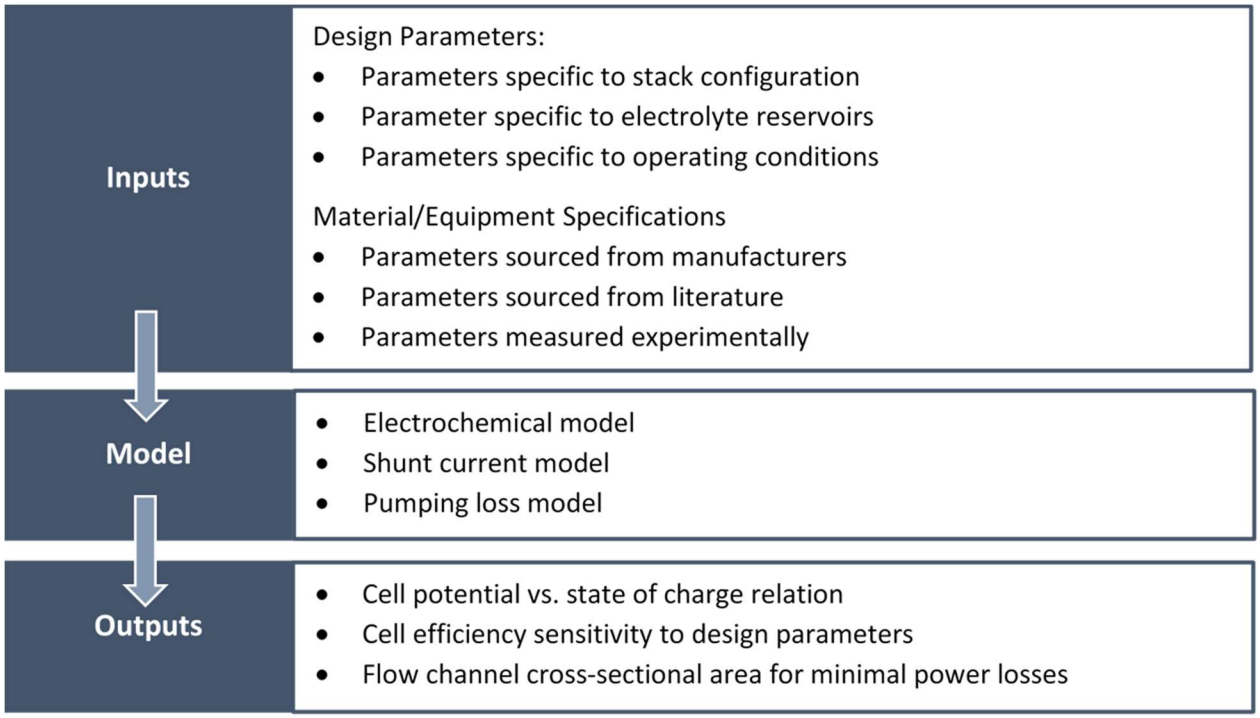

Figure 8-1. High-level model flowchart.

8.1 Inputs

There are two categories of input parameters required by the performance model: design parameters and material specifications. The selection of design parameters comes first logically as well as in the model. After selections for the design parameters are made, additional parameters are needed to account for the specific properties of the materials and equipment chosen.

8.1.1 Design Parameters

Design parameters are broken down into three subcategories: stack configuration, electrolyte reservoirs, and operating conditions. Within each of the subcategories, there are many individual parameters that must be considered individually and specified upfront. There are many stack configuration parameters including the number of cells in the stack, the electrode material choices for both the positive and negative sides, the membrane used, etc. The parameters that must be specified for the electrolyte reservoirs are the composition of the electrolyte (both active species and supporting electrolyte) and the volume of electrolyte in the reservoirs. Operating conditions for the battery include the temperature at which it is operated, the flow rate of electrolyte pumped through the stack, as well as the applied current density.

8.1.2 Material/Equipment Specifications

For equipment and many materials used in the system being modeled, physical properties are provided by the manufacturers. It is prioritized to use the values provided by manufacturers whenever possible. When the needed parameters are not provided by the manufacturer or when an alteration is made to the material, other sources are looked to for the values. The next step taken is a literature search for the needed properties by reliably reported sources. If the needed parameters are not found in literature, experimentation is performed to analyze the properties of interest.

8.2 Model Description

There are three components to the model that each play an integral role in modelling the overall performance of the flow battery system. These components are the electrochemical model, shunt current model, and pumping loss model.

8.2.1 Electrochemical model:

A zero-dimensional electrochemical model is used for the system. A core set of assumptions are made explicitly to initially build the model. As the model is shown to accurately predict the behavior of experimentally tested systems, some assumptions can be addressed and potentially removed to broaden the application of the model. It is designed to function for both symmetric and asymmetric electrode configurations, with possible asymmetries being in electrode material and quantity. The model is also adapted to predict the behavior of systems with mixed acid supporting electrolytes. Cell potential vs. state of charge shown graphically as well as a cell efficiency calculation are the immediate outputs of this component to the performance model.

8.2.2 Shunt current model:

The Shunt current model analyzes the equivalent circuit for the system using the Kirchoff's loop law to obtain the current passing though the channels and manifolds of the stack. Power loss can then be calculated from combining Ohm's law and Watt's law. Finding this component of power loss is the goal of the shunt current model. As the number of cells in the stack is increased, the shunt losses will also increase.

8.2.3 Pumping loss model:

To model the overall pressure drop across the system, both the pressure drop from the electrodes and the flow channels must be accounted for. Darcy's law is be used for the electrodes and the Hagen-Poiseuille equation is used for the flow channels. Since these sources are in series, the individual components can be summed to get the total pressure drop. The ratio of flow rate to pump efficiency can then be multiplied by the pressure drop to obtain the power loss from pumps. Finding this second power loss component is the goal of the pumping loss model.

8.3 Outputs

The outputs of the performance model are designed to be integrated into a cost model of the system

to optimize the balance between technical performance and economic feasibility. The three outputs currently planned for the model are the cell potential versus state of charge relation, the cell efficiency's sensitivity to design parameters, and the optimal flow channel size for minimal power losses.

8.3.1 Cell potential vs. state of charge relation

The electrochemical model directly produces the cell potential vs. state of charge (SOC) relation. It is especially important for the model to fit experimental data well in the SOC range of interest. This output is a primary gauge of model fit to ensure all electrochemical model assumptions are appropriate. Cell efficiency can then be derived from this relation.

8.3.2 Cell efficiency sensitivity to design parameters

There are many design parameters that go into the model and each of them will affect the cell's efficiency differently. Paired with the cost model, knowing the sensitivity of the cell efficiency on each parameter will allow for appropriate prioritization of optimizing efforts. Parameters that can affect the efficiency the most will be a more beneficial focus area than optimizing parameters that have an insignificant impact on efficiency.

8.3.3 Flow channel cross-sectional area for minimal power losses

The flow channel's cross-section area plays a pertinent role in both shunt current losses and pumping losses, but effect each of the two in opposite ways. As the area is increased, the shunt current losses will also increase but the pumping losses will decrease. To minimize overall power losses, an optimal channel size can be determined by the performance model.

9. COST ESTIMATION METHODOLOGY

The owner's costs of constructing and operating an integrated natural gas-fired power plant and battery energy storage system (BESS) will be estimated by constructing a new cost model for the BESS system and integrating it into existing power plant financial models. For the generic reference Cases 1 & 2, costs for baseline powerplant operation will be taken from *Cost And Performance Baseline For Fossil Energy Plants Volume 1: Bituminous Coal And Natural Gas To Electricity (rev 2019).* For the site-specific Cases 3 & 4, cost data will be taken from a 2009 TEA study report generated by an engineering firm which studied the potential upgrading of the plant from a simple cycle to combined cycle. The NETL Power Systems Financial Model MS Excel tool will be utilized to perform the cost calculations. Financial models for these existing power plant cases will be modified as needed to account for cyclical plant operations. In the BESS financial submodel, the losses due to auxiliary loads and inefficiencies of the BESS will be accounted for and determined as a function of charge and discharge rate and state of charge using the BESS performance model described in the prior section. The BESS performance model will also be validated against actual operating data from a laboratory kW-scale test cell stack developed in parallel with this TEA study.

The plant boundary limit is defined as the total plant facility within the "fence line" including fuel receiving and water supply system but terminating at the high voltage side of the main power transformers.

Cost estimates for the power plant portion of the integrated system meet the requirements of an AACE Class 4 Cost Estimate (-15%/+25%), as defined in the NETL report, "Quality Guidelines for Energy System Studies (QGESS): Cost Estimation Methodology for NETL Assessments of Power Plant Performance" (2019) [3]. Cost estimates for the BESS will strive to meet AACE Class 5 (-25% to +50%)

The BESS financial submodel will be guided by the methodologies outlined in the *DOE/EPRI 2013 Electricity Storage Handbook* [4] and the *2020 Grid Energy Storage Technology Cost and Performance Assessment* [5]. Budgetary estimates for capital equipment will be obtained by contacting vendors. Additional methods and component cost information may also be derived from these prior studies [6-8]. The BESS capital cost estimate will be broken down according the major components listed in Section 8. An operational period and expenditure period of 20 years will be assumed for the BESS.

Economic calculations will be performed on a 2020 cost basis. Cost calculated in prior years will be corrected for inflation.

Contingencies: BESS model will include a process contingency (percent of associated process capital) of 20%, consistent with AACE guidelines for technologies proven at the small pilot scale. A project contingency (percent of the sum of BEC, EPC fees, and process contingency) of 15% will be included, typical for a "budget type" AACE Class 4 or 5 estimate [3].

The economic performance evaluation will utilize the global economic assumptions listed in the QGESS.

Cost Metrics to be Calculated:

1. BESS Installed Cost ($/kW)
The installed cost includes all equipment, delivery, installation, interconnection, and step-up transformation costs, divided by the rated discharge capacity.

2. BESS Levelized Cost of Capacity ($/kW-yr)
The levelized cost of capacity is the $/yr revenue per kW of rated discharge capacity needed to cover all life-cycle fixed and variable costs and provide the target rate of return based on financing assumptions and ownership types.

3. BESS Levelized Cost of Storage (LCOS) ($/MWh)
The LCOS is the price for actual delivered energy needed to cover all life-cycle fixed and variable costs, and provide the target rate of return based on financing assumptions and ownership types. LCOS calculation for energy storage is analogous to the LCOE calculation for power generation facilities but uses charging cost as the input "fuel" cost. An assumed number of cycles per year is included, and this metric will also be reported on a per-cycle basis.

4. Integrated Plant Levelized Cost of Electricity (LCOE) ($/MWh)
This is the LCOE of the combined fossil/BESS asset.

REFERENCES

[1] Cost And Performance Baseline For Fossil Energy Plants Volume 1: Bituminous Coal And Natural Gas To Electricity (2019) NETL-PUB-22638 doi:10.2172/1569246.

[2] Kokkinos, A. "Energy Storage for Fossil Fuel Energy Systems". presented at the Thermal-Mechanical-Chemical Energy Storage Workshop, Pittsburgh, PA, February 4, 2020. link.

[3] Quality Guidelines for Energy Systems Studies Cost Estimation Methodology for NETL Assessments of Power Plant Performance (2019) NETL-PUB-22580 doi:10.2172/1567185.

[4] Akhil, A.A., G. Huff, A. B. Currier, B. C. Kaun, D. M. Rastler, S. B. Chen, A. L. Cotter, D. T. Bradshaw, and W. D. Gauntlett, DOE/EPRI 2013 Electricity Storage Handbook in Collaboration with NRECA (2013) SAND2013-5131.

[5] Mongird, K., V. Viswanathan, J. Alam, C. Vartanian, V. Sprenkle, R. Baxter, 2020 Grid Energy Storage Technology Cost and Performance Assessment (2020) DOE/PA-0204.

[6] Viswanathan, V., A. Crawford, D. Stephenson, S. Kim, W. Wang, B. Li, G. Coffey, E. Thomsen, G. Graff, P. Balducci, M. Kintner-Meyer, V. Sprenkle. Cost and performance model for redox flow batteries, Journal of Power Sources 247 (2014) 1040-1051. doi:10.1016/j.jpowsour.2012.12.023

[7] Davies, D.M., Verde, M.G., Mnyshenko, O. et al. Combined economic and technological evaluation of battery energy storage for grid applications. Nat Energy 4, 42–50 (2019). doi:10.1038/s41560-018-0290-1.

[8] Darling, R. M., K. G. Gallagher, J. A. Kowalski, S. Haac, F. R. Brushettad, Pathways to low-cost electrochemical energy storage: a comparison of aqueous and nonaqueous flow batteries. Energy Environ. Sci., 2014,7, 3459-3477. doi: 10.1039/C4EE02158D.

Appendix 5 Techno-Economic Assessment (TEA)

To obtain the mass and energy balances for the cases described in the Design Basis, process models were developed in this project. While an integrated and dynamic process model was envisaged wherein the models for the RFB and the power plant would be fully coupled, it was later determined that separate steady-state models would be sufficient for the economic assessment. The process models that were developed in this project are summarized in the following sections.

RFB Modeling

The structure of a holistic RFB model is described Figure 8-1 in Appendix 4 (Design Basis Report). The focus in this project was on the electrochemical component to the performance model, which is designed to produce the cell efficiency versus state of charge relation output. We have determined from literature that a zero-dimensional model should be sufficient for predicting the behavior of our system. A core set of assumptions have been isolated to initially build the model. It is designed to function for both symmetric and asymmetric electrode configurations, with possible asymmetries being in electrode material and quantity. Cell potential vs. state of charge (SOC) and cell efficiency are the immediate outputs of this component to the performance model. Comparison of predicted and observed trends for cell potential versus SOC is used to gauge model fit to ensure all electrochemical model assumptions are appropriate. Figure 1 shows data comparing the current state of the model to experimental data for one cell configuration.

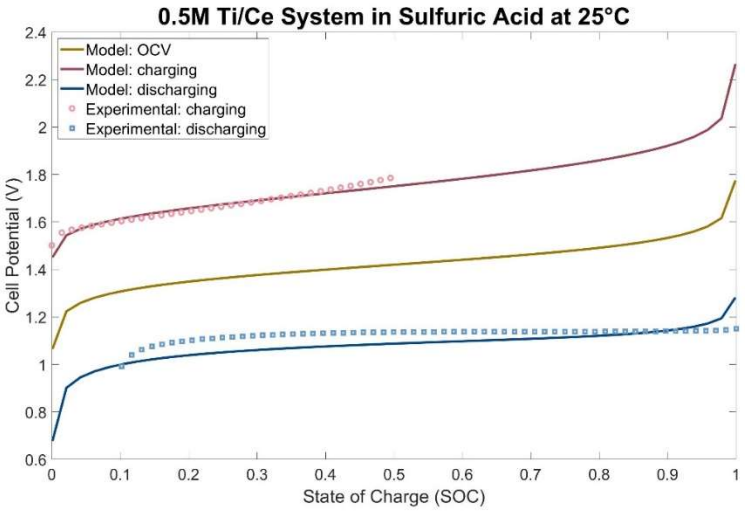

Figure 1. Electrochemical Model Preliminary Data - Positive electrolyte composition: 0.25M Ce2(CO3)3 in 1M H2SO4; Positive electrode: 1 carbon felt; Negative electrolyte composition: 0.5M TiO2SO4 in 1.25M H2SO4; Negative electrode: 1 carbon felt.

The electrochemical model was moved from the build stage to the validation stage. Experimental data from RFB cycling was collected for cell configurations and electrolyte compositions beyond the initial test case used when building the model. Some configurations have shown good fit while others have not. The differences between such cases required further investigation. Sensitivity tests have also been run for the initial test case to gauge which parameters most impact the energy efficiency. Figure 2 shows an example of this where all model parameters are held constant except reaction rate constants, which were manually altered. These sensitivity trends provide guidance as to the most beneficial pathways for electrochemical energy efficiency improvements. Plans for both the shunt current and pumping loss models have been outlined. This includes isolating the initial assumptions and needed parameters. Some parameters required have not been reported in literature and should be determined experimentally.

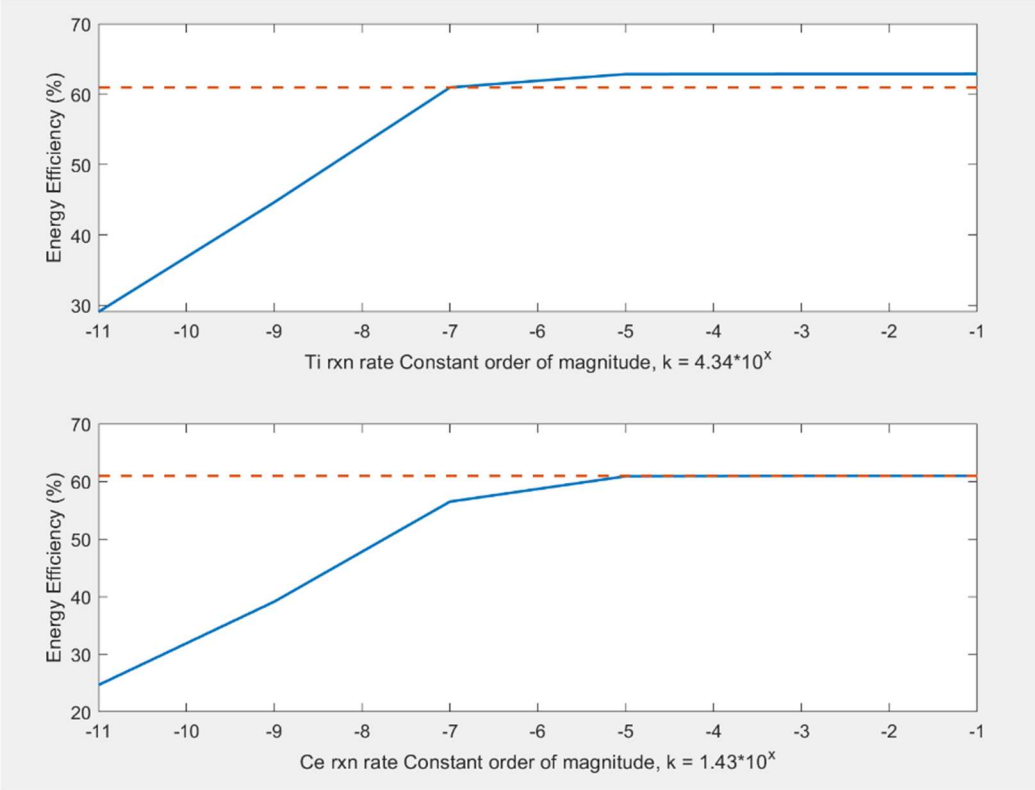

Figure 2. Electrochemical Model Sensitivity to Reaction Kinetics: Positive electrolyte composition: 0.25M Ce2(CO3)3 in 1M H2SO4; Positive electrode: 1 carbon felt; Negative electrolyte composition: 0.5M TiO2SO4 in 1.25M H2SO4; Negative electrode: 1 carbon felt; SOC range 0% to 100%

Power Plant Modeling

Existing process models that were used to develop the reference cases in the NETL Cost and Performance Baseline report (NETL-PUB-22638, 2019) could not be shared due to proprietary data. Therefore, steady-state process models for the natural gas power plant cases were developed from scratch in ASPEN Plus. The purpose of these process models is to predict the plant efficiency (or heat rate) as a function of load. Since deep and frequent cycling of NGCC plants is expected, based on the load profiles presented in the Design Basis, it is important to quantify the costs associated with operating the plant away from its full-load, baseline design conditions so that the economic benefits of adding storage capacity and reduced cycling can be captured.

The ASEPN flowsheet corresponding to a reproduction of NETL Baseline Case 31A: NGCC power plant without carbon capture, is shown in Fig. 3. The model was constructed by referencing the mass and energy balance diagrams found in the NETL Cost and Performance Baseline report (NETL-PUB-22638, 2019). Isentropic efficiencies for compressors and turbines were inferred such that the calculated gross power output of the steam and gas turbines were equal to the NETL-reported values. Some potential inaccuracies in the NETL mass and energy balance diagrams were found. Specifically, the gas turbine outlet temperature listed on the diagram differs from what is listed in the body of the report (1121 F vs 1156 F), and the water/steam mass flows do not appear to be balanced. The ASPEN model was constructed by using the steam temperatures and pressures shown in the diagrams while adjusting the mass flow rates as needed.

An ASPEN model of the Ameren Venice Energy Center (VEC) was also constructed. Performance characteristics for VEC plant components are derived from a prior engineering study report of that plant, which was provided by partner Ameren. Two cases for VEC were developed: a dual combustion gas turbine (simple cycle) arrangement, which is the actual existing plant configuration, and a hypothetical 2 CC x 1 HRSG arrangement. The ASPEN flow sheet for the VEC in the combined cycle configuration is shown in Fig 4.

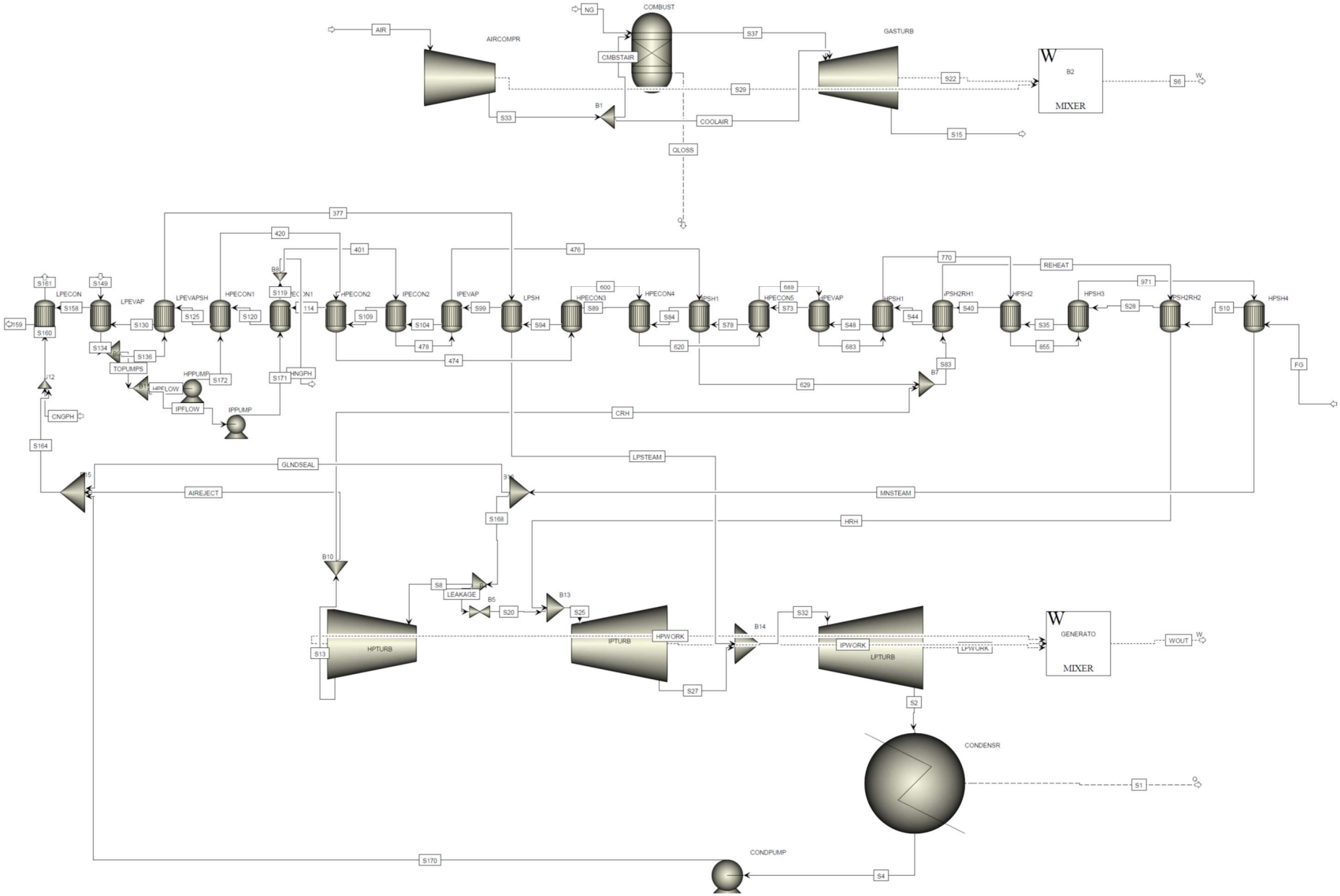

Figure 3. ASPEN flow sheet for reproduction of NETL Baseline Case 31A, natural gas combined cycle power plant.

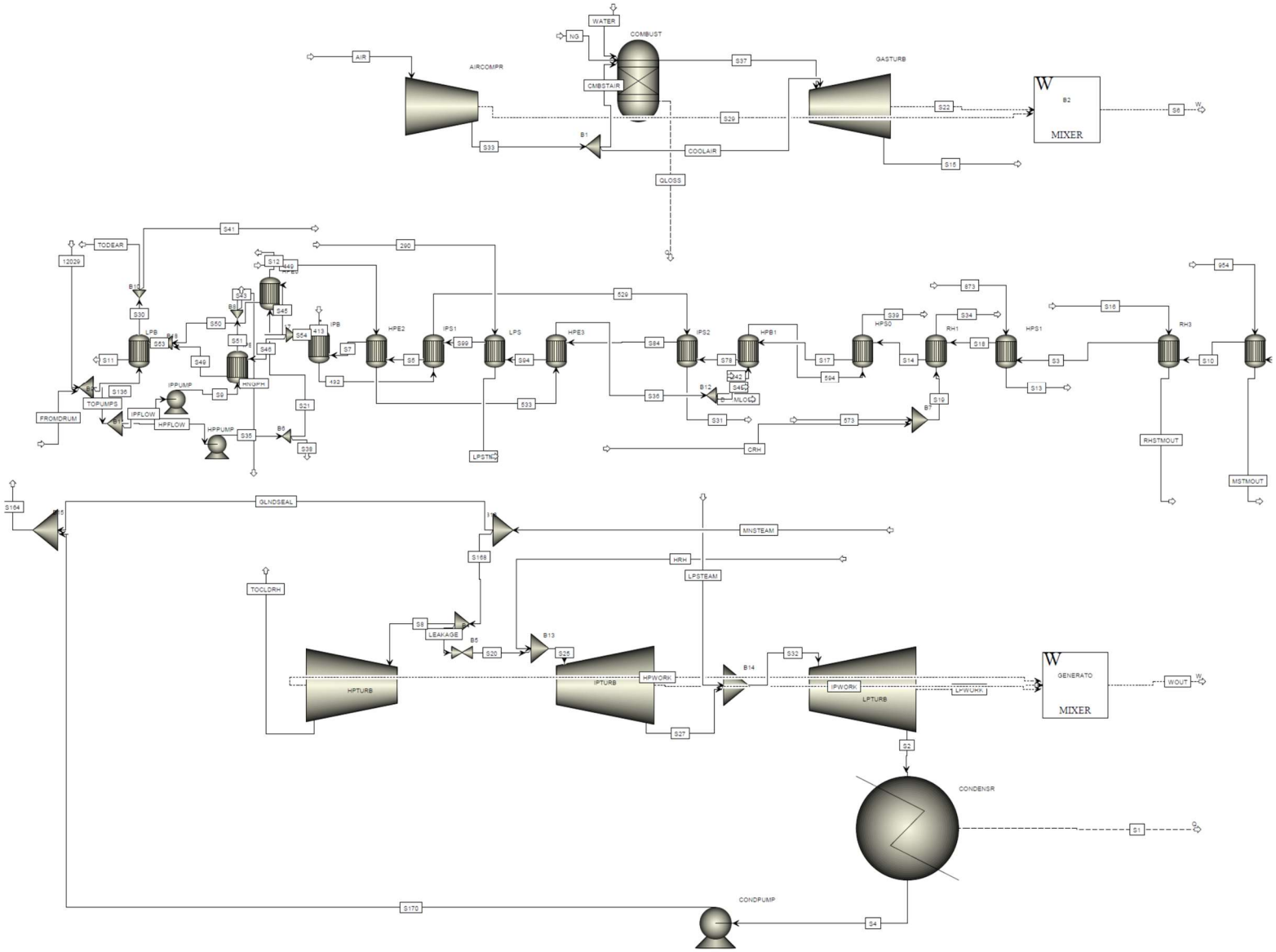

Figure 4 – ASPEN Flowsheet for Venice Energy Center power plant, NGCC configuration

In Table 1, some key gas turbine characteristics and operating parameters of VEC are summarized and compared against those derived for NETL Baseline Case 31A.

Table 1 – Comparison of derived combustion turbine parameters

	Gross Output (MW)	**Pressure Ratio**	**Isentropic Efficiency (%)**	**Turbine Inlet Temp (F)**	**Efficiency LHV (%)**
NETL Baseline Case 31A	238.5 x 2	19.5	87	2470	39.0
Ameren VEC	169 x 2	15.0	87	2300	36.0

Load Profiles: Intermediate Storage Duration

For the short-term duration case (0-2 hours charge/discharge), the capacity of the battery will be relatively small compared to that of the fossil plant and operation of the battery is not expected to significantly impact the operation of the fossil plant. We thus turn attention to the intermediate case (up to 24 hours charge and discharge cycle). To determine the necessary power and energy storage capacities of an integrated RFB system, we further examined the design week-long load profile for the spring, summer, and winter seasons. Figure 5 (left column) shows the overall weekly load profiles (normalized) for a fossil plant in the absence of any storage (grey curve). The plant experiences daily cycling from roughly 40% to 100% capacity. The red curve represents the potential load profile of an integrated RFB, and the blue curve represents the corresponding adjusted load profile for the fossil plant. The objective in is this case, when determining the battery output, was to allow the battery system to handle the bulk of the daily ramping duty, resulting in smoother plant operation over a period of several days. The RFB discharges during the late-day peak in demand and is recharged in the night with power supplied by the fossil plant. The corresponding battery state of charge (SOC) is shown in Figure 5 (right column).

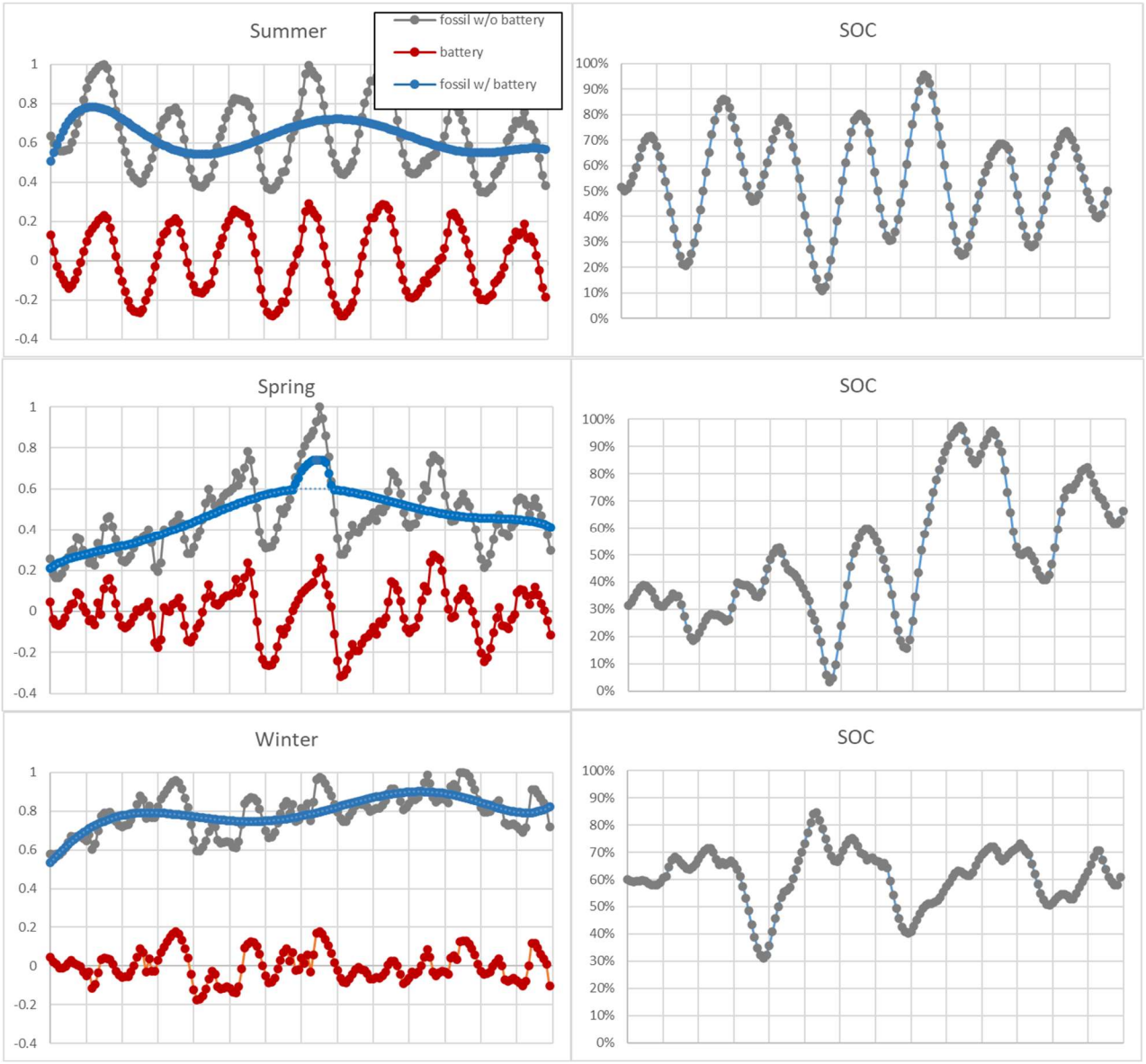

Figure 5 – (left) normalized load profiles with and without RFB integration and (right) corresponding RFB state of charge (SOC).

Effect of Turndown on Plant Efficiency

Prior studies have examined the increased costs on fossil plants due to additional cold starts and early equipment failure due to fatigue (see Section 2 of main body of report). In this work we focus on the economic impact of forced turndown or curtailment when allowing for high fractions of renewable power to enter the grid, to therefore elucidate the economic benefit of this cost avoidance when implementing large-scale storage. Forced turndowns reduces the capacity factor, which increases cost of electricity in two ways: 1) the electricity price required to recover expenses in a given time period is increased due to reduced annual output, and 2) the plant efficiency is reduced when it is operated below the design load, resulting in increased fuel costs.

It was anticipated early in the project that the relationship between the deviation from the design output and the resulting plant efficiency (or heat rate) would need to be derived through extensive ASPEN simulations. But this relationship was recently carefully addressed in a paper by Rezazadeh et al. (2015)[1]. Turndown of an NGCC plant is a complex matter and is limited by minimum airflow required at the main air compressor and the resulting reduced temperature at the turbine outlet. Rezazadeh et al. examined the NETL NGCC reference plants, with and without post combustion capture (PCC). The published data was replotted in Fig 6, which shows the number of percentage points loss in efficiency as a function of the percent plant design capacity. The data was fitted with a 2nd order polynomial.

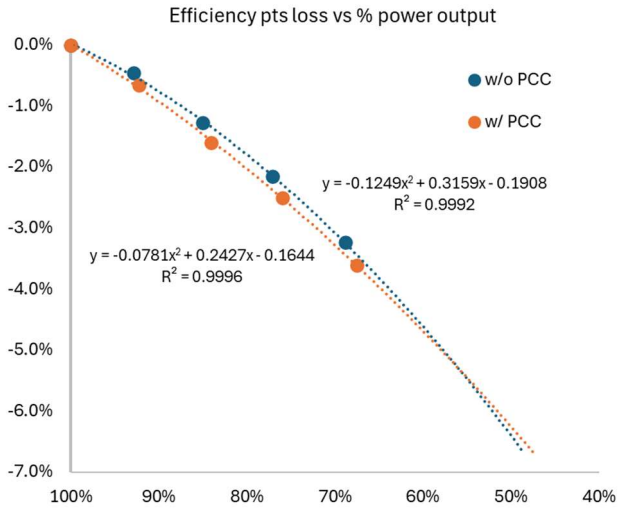

Figure 6. Number of percentage points loss in efficiency (HHV) as a function of the percent plant design capacity. Adapted from[1].

In the NETL power plant model, a capacity factor of 0.85 is assumed in the economic calculations. It is assumed that the plant always operates at the design efficiency, therefore the reduced capacity factor is largely due to scheduled and unscheduled shutdowns. In the following analysis, we assume continuous plant operation and that the capacity factor instead represents deviation from maximum output due to forced turndown. Table 2 shows the resulting annual capacity factor and average plant efficiency (HHV) for the two scenarios represented in Figure 5, i.e. with and without battery storage, for the summer week. In the case with battery storage, it is also assumed that the fossil plant will operate at maximum output when possible (i.e. the fossil load profile is shifted up such the maximum normalized output is at 1.0, and that corresponding baseline load reductions will take place elsewhere, likely from fossil plant retirements).

Table 2. Effect of battery integration on NGCC plant efficiency (Case 31a) in the scenario of high renewable energy

	Capacity Factor	**Average Efficiency (% HHV)**
Without Battery	0.63	49.1
With Battery	0.85	52.3

Battery Sizing

Based on such normalized load profiles, the recommended RFB instantaneous power and energy capacity was calculated for each of the plants considered in this study. Representative results are shown below in Table 3.

Table 3 – Results of Battery Sizing Calculations for the Intermediate Storage Case

Fossil Plant / Size	**Battery Max Power (MW)**	**Battery Capacity (MW-hr)**
1,000 MW	300	3,500
NETL Baseline NGCC: 727 MW	218	2,545
VEC NGCC: 504 MW	151	1,764

Calculations for the electrolyte storage tank capacity requirements were performed. The specific volume requirement (volume of liquid per unit energy stored) can be directly calculated knowing the active solute concentration in the electrolyte solution and the operating voltage. For a "rule of thumb" estimation, one can assume a concentration of 1 M, and an operating potential of 1 V, which results in a volume of approximately ***10 gallons/kWh, per electrolyte***.

This result was compared with publicly available information on the Ronke Power vanadium RFB project, which is reported to be the largest RFB installation in the world that is grid connected (100 MW/400 MWh)[2]. The reported size of Ronke's electrolyte storage tanks associated with their 500 kWh module (Fig 7) was found to be consisted with the above rule of thumb.

A 1,000 MWh facility would require approx. 100,000 gallons of electrolyte (x2). This could be achieved with 200 tanks of 1,000 gallons each. Considering industrial sulfuric acid tanks as a model, such a tank might be 30 ft in diameter with a height of approx. 20 ft. Leaving 10 ft between tanks, the estimated land area required for such a storage facility is 7-8 acres (or roughly 2 city blocks). Figure 8 shows a hypothetical 1,000 MWh installation on a closed coal ash impoundment site at VEC. Larger tank sized could be deployed to reduce the footprint.

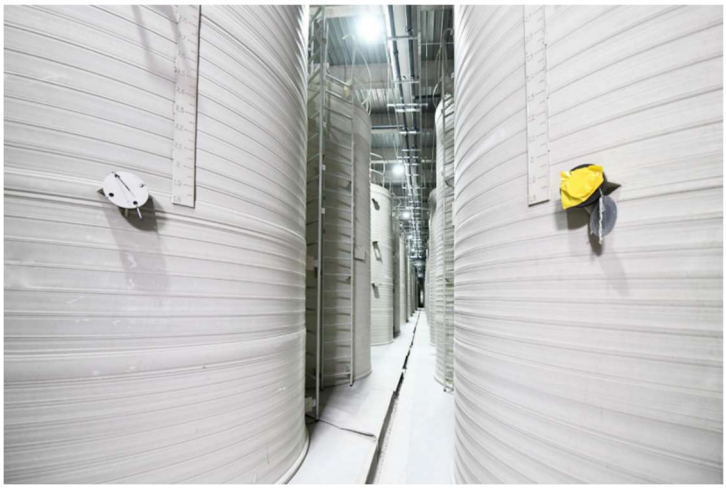

Figure 7. Dalian Flow Battery Energy Storage, Peak-Shaving Power Station 100 MW/400 MWh Rongke Power Co. Ltd. . "World's Largest Flow Battery Energy Storage Station Connected to Grid" Estimated 40,000 gal tank, Qty 100 (x2)

Figure 8. Hypothetical 1,000 MWh Installation at VEC.: 10,000,000 gal, Qty 100 100,000 gal tanks (x2) (Diam 30 ft, Ht 19 ft)

Given the significant footprint required in this medium duration storage case, and considering the limited availablility of open land at existing power plants, it was determined that an integrated installation within a plant fenceline for the long duration case (24-48 hours) would be largely impractical for most plants. We therefore did not further pursue this case for analysis.

Cost Calculations

An existing RFB cost model was updated by UTSA during this project and validated against a PNNL reference model for an all-Vanadium flow battery[3]. The model validation was performed at these conditions: Power – 1MW; Duration – 4h; 1 molar electrolyte solution concentration; 100 mW/cm^2 power density. The cost model for the Ti-Ce system largely follows the approach and assumptions taken by PNNL and the reader is referred to the report for details[3]. The electrolyte costs for the Ti and Ce solutions (in H_2SO_4) as a function of molarity are shown in Fig 9.

The resulting CAPEX cost for the Ti-Ce RFB system is presented in Table 4. Two system sizes are provided. The total AC cost includes the DC storage system plus installation, power transformers and grid connection. This represents a reduction of approx. 80-100 $/kWhr as compared to the all-V system, due to the lower cost of the electrolyte.

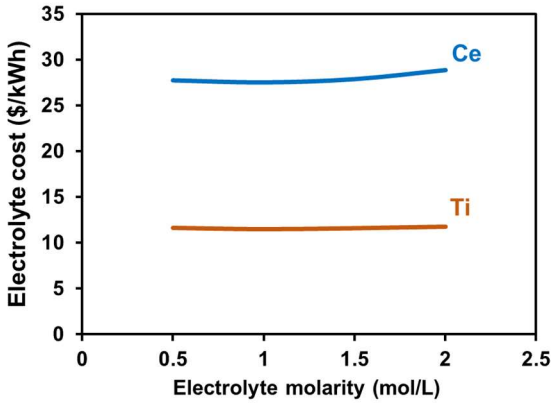

Figure 9. Estimated electrolyte cost as a function of molarity

Table 4 Projected 2030 CAPEX costs for the RFB system

	Ti-Ce RFB		All Vanadium RFB[3]	
	1MW/4MWh	**10MW/40MWh**	**1MW/4MWh**	**10MW/40MWh**
AC total installed ($/kWh)	401	345	487	450

The ideal battery power range for this study (Table 3) was found to be on the order of 100 MW. Analysis by PNNL (Fig 10) best illustrates the effect of duration on the CAPEX. Redox flow batteries, since the power and energy are decoupled, are shown to be one of the most expensive storage options for short durations (0-4 hours). On the other hand, the costs (per kWh) are significantly reduced for longer duration applications (10-24 hrs), making RFBs very competitive with other storage technologies.

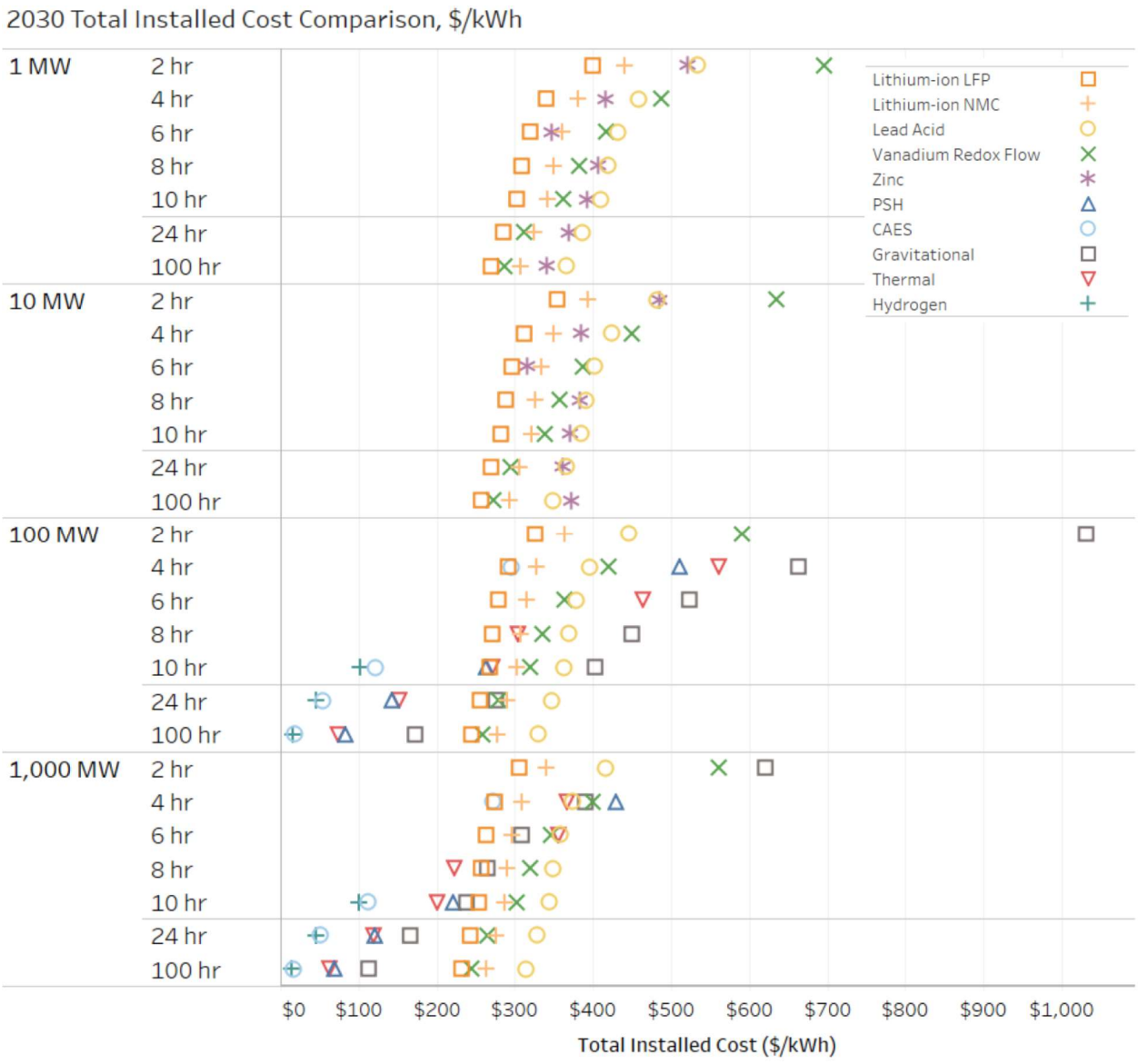

Figure 10: Energy Storage Installed Cost by Technology (reprinted from PNNL-33283)

PNNL also examined the effect of duration on the levelized cost of storage (LCOS). Figure 11 shows that the LCOS is minimized when the storage duration is in the range of 10-12 hours. Therefore, based on these cost models, the projected fossil plant load analysis, and land use, we conclude that the optimal RFB system size should be on the order of 100 MW with a max duration of 12 hours. (1,200 MWh energy).

The LCOS for a Ti-Ce RFB system is estimated to be in the range of 150-200 $/MWh (in 2021 dollars, see Fig 11).

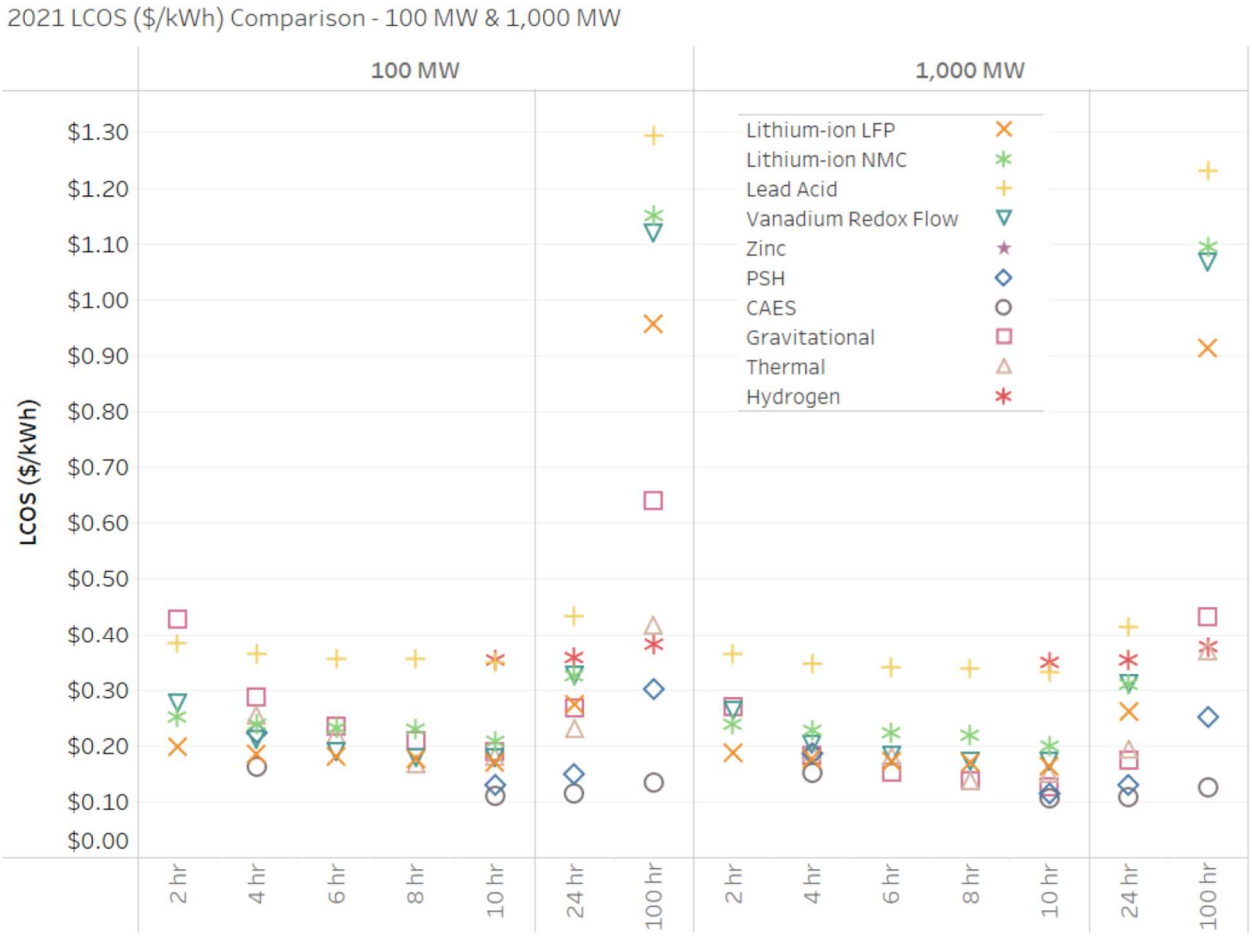

Figure 11: Levelized Cost of Storage by Technology (reprinted from PNNL-33283)

The NETL Power Systems Financial Model was used to calculate the cost of electricity (COE) for the two cases considering NGCC Case 31a described earlier and summarized in Table 2. Costs were escalated from 2018 to 2021 at 3% per year. The results in Table 5 below indicate that the installation of a battery system can reduce the fossil plant standalone COE by $7/MWh, through increased capacity factor and improved average efficiency. While this cost savings is significant from the perspective of the fossil generator, the LCOS of the storage system is an order of magnitude higher than the COE of fossil-fueled power generation. Therefore, we foresee the cycling of fossil plants to increase in the next 5 years, as it is the most economical means of preventing curtailment of new renewable sources considered in this study (increased transmission is another means not considered here). The implementation of such large-scale RFB systems will likely be limited without further government market intervention or changes within the independent grid operating market to incentivize additional reserve capacity. Since flow batteries

are low voltage devices, consideration should also be given to locating such battery systems away from existing power plants and instead at substations where the tie-in voltage is lower, to reduce the grid connection costs associated with step-up voltage transformers.

Table 5. Effect of battery integration on NGCC (Case 31a) COE in the scenario of high renewable energy. COE given in 2021 dollars

	Capacity Factor	**Average Efficiency (% HHV)**	**COE ($/MWh)**
Without Battery	0.63	49.1	$55.26
With Battery	0.85	52.3	$48.06

References

1. Rezazadeh, F., W.F. Gale, K.J. Hughes, M. Pourkashanian, International Journal of Greenhouse Gas Control, 39, 397-406 (2015). 10.1016/j.ijggc.2015.06.003
2. https://english.cas.cn/newsroom/research_news/chem/202205/t20220531_306054.shtml.
3. 2022 Grid Energy Storage Technology Cost and Performance Assessment, PNNL-33283, link to pnnl.gov